



Project Number:	IST-026905
Project Title:	Multiple-Access Space-Time Coding Testbed
Project Coordinator:	C.F. Mecklenbräuker
Deliverable Number:	D1.2.1

Title of Deliverable:	Multi-user space-time code design and database of specific code constructions
Workpackage:	WP-1
Nature:	R
Dissemination level:	PU
Editor:	Yi Hong and Emanuele Viterbo
Authors:	see list inside
Contractual Date of Deliverable:	Jun. 30, 2007
Actual Date of Delivery:	Jun. 30, 2007

Abstract:

This deliverable summarises the obtained novel results in MASCOT Task 1.2 within WP1 on 1) multiuser space-time code design; 2) the joint design of space-time codes and a multiple-input multiple-output (MIMO) multiuser scheme; 3) the joint design of capacity approaching codes and a multiple access scheme; and 4) a low complexity decoding scheme for a MIMO multiuser system.

Contents

1	MU-MIMO Space-Time Code Design	8
1.1	Multuser Space-time Code Design	8
1.1.1	Introduction	8
1.1.2	Channel and Signal Models	9
1.1.3	Characterization of Error Events	10
1.1.4	Code Design Criteria	11
1.1.5	Numerical Example	15
1.2	Outage Analysis of Ricean Fading MIMO Channels	16
1.2.1	Introduction	16
1.2.2	System Model	17
1.2.3	The Notion of a “Critical Rate”	17
1.2.4	Diversity-Multiplexing Tradeoff	19
1.3	Concluding Remarks	24
2	MU-MIMO Downlink Space-Time Block Coded Transmission Scheme	27
2.1	Introduction	27
2.2	System Model	28
2.3	STBCs for MIMO Multuser systems	29
2.3.1	Rank and Determinant Criteria	30
2.3.2	TAST Codes for the Downlink of Multuser MIMO Systems	30
2.3.3	Perfect STBCs for the Downlink of Multuser MIMO Systems	31
2.4	Lattice Decoder for the Downlink of MIMO Multuser systems	32
2.5	Simulation Results	34
2.6	Conclusion	35
3	Spatially Multiplexed LDPC Codes for Multi-User Detection	36
3.1	Introduction	36
3.2	System Description	36
3.2.1	Multi-User Detector	37
3.3	EXIT Functions	38
3.3.1	Coding versus Spreading	40
3.3.2	Multiple Transmit Antennas	41
3.4	LDPC Code Design	42
3.5	Simulation Results	42
3.6	Conclusion	42

4	MU-MIMO Uplink Using IDMA and Low-Complexity Iterative Receivers	45
4.1	Introduction	45
4.2	The Proposed MIMO-IDMA System	46
4.2.1	Basic System Model	46
4.2.2	MIMO-IDMA Transmitter	46
4.2.3	Iterative MIMO-IDMA Receiver	46
4.3	A Low-Complexity Soft Multiuser Detector for MIMO-IDMA	48
4.3.1	Flat-Fading Channel	49
4.3.2	Frequency-Selective Channel	50
4.4	Simulation results	51
4.5	Conclusions	53
5	Conclusions and Recommendation	54

Authors

Yi Hong

Università della Calabria

tel.: +39 338 7092 371

fax.: +39 0984 494713

e-Mail: hong@deis.unical.it

Emanuele Viterbo

Università della Calabria

tel.: +39 0984 494778

fax.: +39 0984 494713

e-Mail: viterbo@deis.unical.it

Executive Summary

The aim of Task 1.2 within the MASCOT project is the design of multiuser space-time codes, the efficient multiple-input multiple-output (MIMO) multiple access scheme, and the efficient decoding scheme for multiuser systems. This deliverable provides the relevant technical contributions and assessment of their performance in quantitative terms with specific focus on the following topics.

1. (**Design of multiuser space-time codes:**) Chapter 1 successfully explored the space-time/frequency coding for multiple-access channels (MACs). Starting from an information theoretic point of view, the rate-dependent space-time/frequency code design criteria for fading multiantenna MACs are derived. It is demonstrated that, depending on the transmission rate tuple, joint designs taking the presence of multiple users explicitly into account may be necessary. The results allow to identify the rate regions where, for each user, employing codes designed for the single-user case is optimal. Also, the number of receive antennas plays an important role in the code design criteria.

The outage characteristics of correlated Ricean fading, coherent MIMO channels are analyzed. Finally, Chapter 1 provides a complete characterization of the optimum diversity-multiplexing tradeoff for correlated Ricean fading MIMO channels taking into account the existence of the critical rate and thereby establishing the notion of a critical multiplexing gain.

2. (**Design of space-time coded MIMO multiuser transmission scheme:**) Chapter 2 considers the downlink of a space-time block coded multiuser MIMO system. An efficient multiuser transmission scheme is developed, where the threaded algebraic space-time block codes and perfect space-time block codes are used to separate the data streams of the multiple users. After despreading the signal sequence at the receiver of each user, the maximum likelihood decoding is obtained by a lattice decoder. This transmission scheme has the advantage of supporting the highest possible data rate and full diversity of the multiuser MIMO systems.
3. (**Joint design of capacity approaching codes and a multiple access scheme:**) From an information theoretic point of view, Chapter 3 provides the analysis of the extrinsic information transfer function of multi-user detection (MUD) for synchronous Code Division Multiple Access (CDMA) with various loads and the signal to noise ratio. This transfer function is used to discuss the benefits of putting redundancy into spreading or coding. Finally, it is shown how low-density parity-check codes can be designed for a specific system.

4. (**Design of a low complexity decoding scheme for a MIMO multiuser system:**) Chapter 4 considers practical relevant issues of low complexity decoding scheme for an Interleave-division multiple access (IDMA) MIMO system. The IDMA system has recently been proposed as an alternative to CDMA. The novelty of IDMA lies in the combination of the low rate channel coding in place of spreading, and soft-in soft-out multiuser detectors with reduced complexity. User specific interleavers are used as a tool to separate users at the receiver. Chapter 4 provides the extension of the IDMA to MIMO multiuser systems employing spatial multiplexing. An low complexity iterative receiver for MIMO-IDMA is developed with great potential for future hardware implementation.

Acknowledgement

All technical contents of the Deliverable 1.2.1 of the MASCOT project can be also found in the following publications. We acknowledge all the authors.

1. M.E. Gärtner and H. Bölcskei, “Multiuser space–time/frequency code design,” in *Proc. IEEE Int. Symp. Inform. Theory (ISIT)*, pp. 2819–2823, Seattle (WA), USA, July 9–14, 2006.
2. M.E. Gärtner and H. Bölcskei, “On the critical rate in Ricean MIMO channels,” in *Proc. IEEE Int. Symp. Inform. Theory (ISIT)*, Nice, France, June 24–29, 2007.
3. Y. Hong, E. Viterbo, and J.-C. Belfiore, “A space–time block coded multiuser MIMO downlink transmission scheme,” in *Proc. IEEE Int. Symp. Inform. Theory (ISIT)*, pp. 257–261, Seattle (WA), USA, July 9–14, 2006.
4. G. Lechner, A.P. Burg, “Design of spatially multiplexed LDPC codes for multiuser detection,” to appear in *Proc. European Signal Processing Conference (EUSIPCO-2007)*, Poznan, Poland, September 3–7, 2007.
5. C. Novak, F. Hlawatsch, and G. Matz, “MIMO–IDMA: Uplink multiuser MIMO communications using interleave division multiple access and low–complexity iterative receivers,” in *Proc IEEE International Conference on Acoustics, Speech, and Signal Processing (ICASSP)*, Vol. 3, pp. III-225–III-228, Honolulu (HI), USA, April 15–20, 2007.

Chapter 1

MU-MIMO Space-Time Code Design

1.1 Multiuser Space-time Code Design

1.1.1 Introduction

The design of space-time/frequency codes for single-user multiantenna channels has been studied in great detail [2, 3, 4, 5]. Little is known, however, about space-time/frequency coding in multiple-access channels (MACs). Past work focuses mostly on employing single-user space-time codes for each of the users and separating the users in signal space [6] or canceling multiuser interference [7]. These approaches lead, however, to (significantly, if the number of users is high) reduced transmission rate [6] or suboptimum performance [7].

A systematic study of the general problem of space-time/frequency code design for MACs seems to be missing. Filling this gap is the main goal of the present paper. Our analysis is based on an idea by Gallager [8], used to characterize the error mechanisms in *two-user* additive white Gaussian noise (AWGN) MACs. Depending on the transmission rate tuple, it is shown in [8] that the dominant error event is either one of the two users or both users being in error. Taking our cue from the results in [8], we can conclude that the rate regions where single-user error events dominate can be dealt with using space-time/frequency codes designed for the single-user case, such as those in [2, 3, 4]. The rate region where the event of both users (or a subset of the users in the case of MACs with more than two users) being in error dominates requires, however, new design criteria as shown in this paper.

An important conceptual difference between the setup in [8] and the case considered here originates from the fading nature of the channel, which results in two sources of errors, namely errors due to additive noise (also present in the AWGN case) and errors due to the channel being in outage. Throughout the paper, we assume that the blocklengths are large enough for errors due to outage to dominate the error performance.

For the sake of simplicity of exposition, we restrict ourselves to the two-user case. Comments on the generalization of our results to the case of an arbitrary number of users will be made where appropriate. Furthermore, we assume that the receiver has perfect channel state information (CSI).

Contributions: The detailed contributions in this Chapter can be summarized as follows:

- We characterize the dominant error event regions for fading multiantenna MACs and discuss their dependence on SNR and the number of antennas at the receiver.
- Based on the dominant error event regions, we establish space-time/frequency code design criteria for fading multiantenna MACs.
- We illustrate the value of code designs taking the multiuser nature of the problem explicitly into account.

Notation: The superscripts T , H and $*$ stand for transposition, conjugate transposition and elementwise conjugation, respectively. \mathbf{I}_N is the $N \times N$ identity matrix, $\mathbf{0}$ is the all-zeros matrix of appropriate size, $\|\mathbf{x}\|$ stands for the Euclidean norm of the vector \mathbf{x} and $\|\mathbf{A}\|_F$ denotes the Frobenius norm of the matrix \mathbf{A} . For an $M \times N$ matrix $\mathbf{A} = [\mathbf{a}_1 \ \mathbf{a}_2 \ \cdots \ \mathbf{a}_N]$, we define $\text{vec}\{\mathbf{A}\} = [\mathbf{a}_1^T \ \mathbf{a}_2^T \ \cdots \ \mathbf{a}_N^T]^T$. If \mathcal{L} is a set, then $|\mathcal{L}|$ denotes its cardinality. $\mathcal{E}[\cdot]$ represents the expectation operator. A multivariate, circularly symmetric, complex Gaussian random vector is a random vector $\mathbf{z} = \mathbf{x} + j\mathbf{y} \sim \mathcal{CN}(\mathbf{0}, \mathbf{\Sigma})$, where the real-valued random vectors \mathbf{x} and \mathbf{y} are jointly Gaussian, $\mathcal{E}[\mathbf{z}] = \mathbf{0}$, $\mathcal{E}[\mathbf{z}\mathbf{z}^H] = \mathbf{\Sigma}$, and $\mathcal{E}[\mathbf{z}\mathbf{z}^T] = \mathbf{0}$. The notation $\mathbf{x} \preceq \mathbf{y}$ for $\mathbf{x}, \mathbf{y} \in \mathbb{R}^N$ with $\sum_{k=1}^N x_k = \sum_{k=1}^N y_k$ means that \mathbf{y} majorizes \mathbf{x} , i.e., $\sum_{k=1}^n x_k \leq \sum_{k=1}^n y_k$ ($n = 1, 2, \dots, N-1$) for the elements of \mathbf{x} and \mathbf{y} being arranged in nonincreasing order. Logarithms are to the base e unless stated otherwise.

1.1.2 Channel and Signal Models

Channel Model

We assume that each of the two users is equipped with M_T transmit antennas and the receiver employs M_R antennas. The matrix-valued fading channel between the two users and the receiver is assumed frequency-selective fading with the $M_R \times 2M_T$ transfer function given by

$$\begin{aligned} \overline{\mathbf{H}}(e^{j2\pi\theta}) &= [\mathbf{H}_1(e^{j2\pi\theta}) \quad \mathbf{H}_2(e^{j2\pi\theta})] \\ &= \sum_{l=0}^{L-1} \overline{\mathbf{H}}[l] e^{-j2\pi l\theta}, \quad 0 \leq \theta < 1. \end{aligned}$$

Here, $\mathbf{H}_i(e^{j2\pi\theta}) = \sum_{l=0}^{L-1} \mathbf{H}_i[l] e^{-j2\pi l\theta}$ ($i = 1, 2$) represents the $M_R \times M_T$ channel between user i and the receiver and $\overline{\mathbf{H}}[l] = [\mathbf{H}_1[l] \ \mathbf{H}_2[l]]$. The channel is purely Rayleigh fading, i.e., $\text{vec}\{\mathbf{H}_i[l]\} \sim \mathcal{CN}(\mathbf{0}, \sigma_i^2 \mathbf{I}_{M_T M_R}) \ \forall l$ for $i = 1, 2$, with the individual taps being uncorrelated (also across users). The path gains σ_i^2 are normalized such that $\sum_{l=0}^{L-1} \sigma_l^2 = 1$. Throughout the paper, the receiver is assumed to have perfect knowledge of both users' channels, whereas the transmitters do not have any CSI.

Signal Model

For simplicity, we assume an N -periodic signal model, which means that the impact of the channel on the transmitted signal is described by circular convolution rather than

linear convolution. Such a signal model is obtained, for instance, when each of the users employs orthogonal frequency-division multiplexing (OFDM) [9] and the cyclic prefix (guard interval) length exceeds the channel order. Denoting the number of OFDM tones as N (where $N \geq 2M_T L$ is assumed throughout), the received vector signal on the n th tone is given by

$$\mathbf{y}^{(n)} = \sqrt{\frac{P}{2}} \overline{\mathbf{H}}(e^{j2\pi \frac{n}{N}}) \overline{\mathbf{c}}^{(n)} + \mathbf{z}^{(n)}, \quad n = 0, 1, \dots, N-1$$

where $\overline{\mathbf{c}}^{(n)} = [(\mathbf{c}_1^{(n)})^T (\mathbf{c}_2^{(n)})^T]^T$ with the $M_T \times N$ codewords $\mathbf{C}_i = [\mathbf{c}_i^{(0)} \mathbf{c}_i^{(1)} \dots \mathbf{c}_i^{(N-1)}]$ ($i = 1, 2$) transmitted by user i and the noise vector (uncorrelated across tones and users) $\mathbf{z}^{(n)} \sim \mathcal{CN}(\mathbf{0}, N_0 \mathbf{I}_{M_R}) \forall n$.

The codewords \mathbf{C}_i ($i = 1, 2$) with $\mathcal{E}[\|\mathbf{C}_i\|_F^2] = N$ are chosen from the codebook \mathcal{C}_i of size M_i according to a given probability assignment. We emphasize that although the users cannot cooperate in selecting their codewords, their codebooks can still be designed jointly, i.e., the design can take the multiuser nature of the problem explicitly into account (cf. the last paragraph in Section 1.1.4). This observation will turn out to be crucial later when dealing with rate tuples that lie in the region where the dominant error event corresponds to both users being in error.

1.1.3 Characterization of Error Events

Upper Bound on Error Probability

As already mentioned in the introduction, the space-time/frequency code design criteria will depend on the individual users' data rates R_i ($i = 1, 2$). We therefore need to first relate the error probability to the rate tuple (R_1, R_2) . The receiver employs joint maximum likelihood (ML) decoding according to

$$\widehat{\overline{\mathbf{C}}} = \arg \min_{\overline{\mathbf{C}}} \sum_{n=0}^{N-1} \left\| \mathbf{y}^{(n)} - \sqrt{\frac{P}{2}} \overline{\mathbf{H}}(e^{j2\pi \frac{n}{N}}) \overline{\mathbf{c}}^{(n)} \right\|^2$$

with $\overline{\mathbf{C}} = [\mathbf{C}_1^T \mathbf{C}_2^T]^T$ and $\widehat{\overline{\mathbf{C}}} = [\widehat{\mathbf{C}}_1^T \widehat{\mathbf{C}}_2^T]^T$. An error occurs, whenever the decision is made in favor of a codeword tuple $(\widehat{\mathbf{C}}_1, \widehat{\mathbf{C}}_2) \neq (\mathbf{C}_1, \mathbf{C}_2)$. In line with the reasoning in [8], we can identify three types of error events, namely errors of type 1 and 2, where only the codeword of user 1 or 2, respectively, is in error and of type 3, where both users' codewords are decoded erroneously. Denoting the corresponding error probabilities as $P_{ek|H}$ ($k = 1, 2, 3$), the total average (w.r.t. the random channel) error probability is given by

$$P_e = P_{e1} + P_{e2} + P_{e3} \quad (1.1)$$

where $P_{ek} = \mathcal{E}_H[P_{ek|H}]$. Depending on the desired transmission rate tuple (R_1, R_2) , one of the three terms in (1.1) dominates the total error probability P_e , leading to the dominant error event regions depicted in Fig. 1.1 and defined as follows: P_{ek} dominates in region $k = 1, 2, 3$. If P_{e1} or P_{e2} dominate, employing, for each of the two users, codes designed

for single-user channels is sufficient. Moreover, these codes can be chosen independently of each other. If P_{e3} dominates, a joint design of the two users' codebooks is required. The notion of a joint design will be made precise in Section 1.1.4.

Exact expressions for the error probability in (1.1) as a function of (R_1, R_2) are difficult to obtain so that we resort to the standard upper bound in terms of error exponents. Setting $R_3 = R_1 + R_2$ in the remainder of the paper, we obtain

$$P_{ek|H} \leq e^{-NE_{rk}(R_k, \bar{\mathbf{H}})}, \quad k = 1, 2, 3$$

where the random coding exponent $E_{rk}(R_k, \bar{\mathbf{H}})$ ($k = 1, 2, 3$) is given by

$$E_{rk}(R_k, \bar{\mathbf{H}}) = \max_{0 \leq \tau \leq 1} \max_Q (E_{0k}(\tau, Q, \bar{\mathbf{H}}) - \tau R_k)$$

with $E_{0k}(\tau, Q, \bar{\mathbf{H}})$ being defined (replacing $P(\mathbf{Y}|\bar{\mathbf{C}})$ by $P(\mathbf{Y}|\bar{\mathbf{C}}, \bar{\mathbf{H}})$) as in [8, Th. 2]. Furthermore, Q denotes the probability assignment on the transmitted codeword matrices.

The probability density function of $E_{rk}(R_k, \bar{\mathbf{H}})$ (note that $\bar{\mathbf{H}}$ is random) has a nonzero probability mass at $E_{rk}(R_k, \bar{\mathbf{H}}) = 0$, because the random coding exponent becomes zero for all channel realizations $\bar{\mathbf{H}}$ that do not support the desired rate R_k (due to outage). This observation, combined with the long blocklength assumption (the blocklength is assumed large enough so that errors due to additive noise can be ignored [10]) made earlier, results in (the outage probability)

$$P_{ek} = P(E_{rk}(R_k, \bar{\mathbf{H}}) = 0). \quad (1.2)$$

The Case of Gaussian Codebooks

The purpose of this subsection is to discuss the dependence of the dominant error event regions on M_R and $\text{SNR} = P/N_0$. For Gaussian codebooks (which are capacity achieving), $M_T = 2$, $L = 1$, and various choices of M_R and SNR , Fig. 1.1 shows the dominant error event regions (obtained by means of Monte-Carlo simulations from (1.2)).

We observe that for fixed SNR , increasing M_R results in a reduction of the relative size of the region where both users are in error (region 3). This is due to the fact that for large M_R there are more spatial degrees of freedom and hence, imposing "separation" through appropriate joint code design is required only for a small set of (high) rates. From Fig. 1.1, we can infer that this effect is much less pronounced for low SNR , where the concept of spatial separation is not relevant [11]. In summary, we can conclude that increasing M_R results in choosing single-user codes for each of the two users being optimal in a larger fraction of the entire rate region. In case of a general number of users, error events corresponding to any subset of users being in error can dominate and code design has to account for that (cf. the last paragraph in Section 1.1.4). Finally, we note that L has hardly any impact on the shape of the dominant error event regions.

1.1.4 Code Design Criteria

As suggested by the results in the previous section, the code design criteria depend on the transmission rate tuple (R_1, R_2) . In order to state the general design guideline, we first need to establish the corresponding rate-dependent code design criteria.

We assume that the codeword matrices are composed of elements drawn from finite scalar constellations. Defining $M_1 = |\mathcal{C}_1|$, $M_2 = |\mathcal{C}_2|$ and $M_3 = M_1 M_2$, the corresponding maximum transmission rates R_k^0 (in nats per tone) are given by $R_k^0 = (1/N) \log M_k$ ($k = 1, 2, 3$).

The expression in (1.2) does not lead to analytically tractable design criteria. Instead, we resort to cutoff rates by choosing $\tau = 1$, which yields

$$E_{\tau k}(R_k, \bar{\mathbf{H}}) \geq E_{0k}(1, Q, \bar{\mathbf{H}}) - R_k \quad (1.3)$$

for arbitrary Q . Using (1.3) in (1.2), we obtain

$$P_{ek} \leq \mathbb{P} \left(\frac{1}{\widetilde{M}_k} \sum_{\substack{\mathbf{C}_k, \mathbf{E}_k \\ \mathbf{C}_k \neq \mathbf{E}_k}} e^{-\frac{\rho}{4} \sum_{n=0}^{N-1} \|\mathbf{H}_k(e^{j2\pi \frac{n}{N}})(\mathbf{c}_k^{(n)} - \mathbf{e}_k^{(n)})\|^2} \geq e^{N(R_k^0 - R_k)} \right), \quad k = 1, 2, 3 \quad (1.4)$$

where we define $\rho = \frac{P}{2N_0}$, $\widetilde{M}_1 = M_1 - 1$, $\widetilde{M}_2 = M_2 - 1$, $\widetilde{M}_3 = \widetilde{M}_1 \widetilde{M}_2$, $\mathbf{H}_3 = \bar{\mathbf{H}}$, $\mathbf{C}_3 = \bar{\mathbf{C}}$ and $\mathbf{E}_3 = \bar{\mathbf{E}} = [\mathbf{E}_1^T \ \mathbf{E}_2^T]^T$. The notation $\mathbf{C}_3 \neq \mathbf{E}_3$ means that both $\mathbf{C}_1 \neq \mathbf{E}_1$ and $\mathbf{C}_2 \neq \mathbf{E}_2$. Furthermore, we define $\mathbf{C}_k = [\mathbf{c}_k^{(0)} \ \mathbf{c}_k^{(1)} \ \dots \ \mathbf{c}_k^{(N-1)}]$ and $\mathbf{E}_k = [\mathbf{e}_k^{(0)} \ \mathbf{e}_k^{(1)} \ \dots \ \mathbf{e}_k^{(N-1)}]$ for $k = 1, 2, 3$. The upper bound in (1.4) requires tightening the corresponding bound in [12, Th. 5.6.1], which is achieved by proper choice of Q (details are omitted due to length constraints). We are now ready to state

Theorem 1. *The error probability P_{ek} ($k = 1, 2, 3$) is upper-bounded according to*

$$P_{ek} \leq \sum_{\substack{\mathbf{C}_k, \mathbf{E}_k \\ \mathbf{C}_k \neq \mathbf{E}_k}} \mathbb{P} \left(\frac{1}{N} \sum_{n=0}^{N-1} \chi_n \lambda_n(\mathbf{R}_k) \leq \frac{4}{\rho} R_k \right)$$

where the χ_n are independent χ^2 -distributed random variables with $2M_R$ degrees of freedom each and $\lambda_n(\mathbf{R}_k)$ stands for the n th eigenvalue of the matrix

$$\mathbf{R}_k = \mathbf{G}(\mathbf{C}_k, \mathbf{E}_k) \mathbf{G}^H(\mathbf{C}_k, \mathbf{E}_k) \quad (1.5)$$

with the stacked codeword difference matrix

$$\mathbf{G}(\mathbf{C}_k, \mathbf{E}_k) = \begin{bmatrix} \sigma_0(\mathbf{C}_k - \mathbf{E}_k)^T & \sigma_1 \mathbf{D}(\mathbf{C}_k - \mathbf{E}_k)^T & \dots \\ \dots & \sigma_{L-1} \mathbf{D}^{L-1}(\mathbf{C}_k - \mathbf{E}_k)^T \end{bmatrix}$$

where $\mathbf{D} = \text{diag}_{n=0}^{N-1} \{e^{-j2\pi n/N}\}$.

Remark: Note that (1.5) can equivalently be expressed in the ‘‘time domain’’ by defining $\mathbf{C}_k^t = \mathbf{C}_k \mathbf{F}$ and $\mathbf{E}_k^t = \mathbf{E}_k \mathbf{F}$ with the $N \times N$ FFT matrix $[\mathbf{F}]_{m,n} = (1/\sqrt{N}) e^{j2\pi mn/N}$

($m, n = 0, 1, \dots, N-1$) and noting that due to unitary equivalence $\lambda_n(\mathbf{R}_k) = \lambda_n(\mathbf{R}_k^t)$ ($n = 0, 1, \dots, N-1$), where $\mathbf{R}_k^t = \mathbf{G}^t(\mathbf{C}_k^t, \mathbf{E}_k^t) (\mathbf{G}^t(\mathbf{C}_k^t, \mathbf{E}_k^t))^H$ with

$$\mathbf{G}^t(\mathbf{C}_k^t, \mathbf{E}_k^t) = \begin{bmatrix} \sigma_0(\mathbf{C}_k^t - \mathbf{E}_k^t)^T & \sigma_1(\mathbf{C}_k^{t-1} - \mathbf{E}_k^{t-1})^T & \dots \\ \dots & \sigma_{L-1}(\mathbf{C}_k^{t-L+1} - \mathbf{E}_k^{t-L+1})^T \end{bmatrix}$$

where \mathbf{C}_k^{t-l} and \mathbf{E}_k^{t-l} denote the matrices obtained by cyclically shifting the columns of \mathbf{C}_k^t and \mathbf{E}_k^t by l positions to the right.

Proof. We start by noting that

$$\mathbb{P}\left(\sum_{i=1}^n e^{-x_i} \geq c\right) \leq \sum_{i=1}^n \mathbb{P}\left(x_i \leq \log \frac{n}{c}\right)$$

which, when applied to (1.4), yields

$$\begin{aligned} P_{ek} &\leq \sum_{\substack{\mathbf{C}_k, \mathbf{E}_k \\ \mathbf{C}_k \neq \mathbf{E}_k}} \mathbb{P}\left(\frac{1}{N} \sum_{n=0}^{N-1} \left\| \mathbf{H}_k(e^{j2\pi \frac{n}{N}}) (\mathbf{c}_k^{(n)} - \mathbf{e}_k^{(n)}) \right\|^2\right. \\ &\quad \left. \leq \frac{4}{\rho} R_k\right). \end{aligned}$$

A straightforward manipulation reveals that the quantity

$$\sum_{n=0}^{N-1} \left\| \mathbf{H}_k(e^{j2\pi \frac{n}{N}}) (\mathbf{c}_k^{(n)} - \mathbf{e}_k^{(n)}) \right\|^2$$

has the same distribution as the quadratic form $\mathbf{h}_w^H (\mathbf{R}_k \otimes \mathbf{I}_{M_R}) \mathbf{h}_w$ with $\mathbf{h}_w \sim \mathcal{CN}(\mathbf{0}, \mathbf{I}_{M_R N})$. Since each nonzero eigenvalue of the matrix $(\mathbf{R}_k \otimes \mathbf{I}_{M_R})$ has multiplicity M_R , the proof is complete.

We shall next consider the high and low-SNR cases, which allows us to formulate tangible code design criteria.

High-SNR Design Criteria

We start with the following

Corollary 2. *Define*

$$P_{ek}(\mathbf{R}) = \mathbb{P}\left(\frac{1}{N} \sum_{n=0}^{N-1} \chi_n \lambda_n(\mathbf{R}) \leq \frac{4}{\rho} R_k\right) \quad (1.6)$$

and let $\boldsymbol{\lambda}_1, \boldsymbol{\lambda}_2 \in \mathbb{R}^N$ be vectors containing the eigenvalues of the positive-semidefinite matrices \mathbf{R}_1 and \mathbf{R}_2 , respectively. If ρ is large, the following holds

$$\boldsymbol{\lambda}_1 \preceq \boldsymbol{\lambda}_2 \Rightarrow P_{ek}(\mathbf{R}_1) \leq P_{ek}(\mathbf{R}_2).$$

Proof. The corollary is a direct consequence of the Schur-convexity of $P_{ek}(\mathbf{R})$ in the vector of eigenvalues $\boldsymbol{\lambda}$ of \mathbf{R} for large ρ [13, Th. 2].

As a consequence of Corollary 2, it can be shown¹ that (keeping R_k fixed)

$$\lim_{\rho \rightarrow \infty} \frac{\log P_{ek}(\mathbf{R})}{\log \rho} = -\text{rank}\{\mathbf{R}\}M_R$$

which implies that the high-SNR error probability P_{ek} is dominated by the codeword difference matrices \mathbf{R}_k with minimum rank. In the high-SNR regime, the space-time/frequency code design criteria minimizing $P_e = P_{e1} + P_{e2} + P_{e3}$ can now be summarized as follows:

1. Given the rate tuple (R_1, R_2) , determine the type ($k = 1, 2, 3$) of error event dominating the overall error probability P_e .
2. If the dominant error event is of type k ($k = 1, 2, 3$), the corresponding error probability P_{ek} is minimized by codes that fulfill:
 - (a) *Rank criterion:* For every codeword pair $(\mathbf{C}_k, \mathbf{E}_k)$ with $\mathbf{C}_k \neq \mathbf{E}_k$ the rank of the corresponding codeword difference matrix \mathbf{R}_k shall be maximized.
 - (b) *Eigenvalue criterion:*² For every codeword pair $(\mathbf{C}_k, \mathbf{E}_k)$ with $\mathbf{C}_k \neq \mathbf{E}_k$ the vector of eigenvalues of the corresponding matrix \mathbf{R}_k shall be majorized by any other possible choice of eigenvalues.

Before discussing the implications of the design criteria above, we note that space-time/frequency codes designed for the single-user case according to 2a) and 2b) are also optimal w.r.t. the classical (rate-independent) space-time/frequency code design criteria [2, 3, 4]. This can be seen by noting that the product of eigenvalues (i.e., the determinant of \mathbf{R}_k) is a Schur-concave function [14, Th. 3.C.1] and hence, an optimum vector of eigenvalues according to 2b) is optimal w.r.t. the determinant criterion in [2] as well. It is interesting to observe that a completely different derivation (as compared to [2, 3, 4]) aiming at minimizing the probability of encountering a bad effective channel³ realization results in essentially the same criteria as those based on pairwise error probability [2, 3, 4].

Joint code design: If the rate tuple (R_1, R_2) lies in the dominant error event region 1 or 2, we design codes according to the criteria 2a) and 2b) for each of the two users. The two codebooks can furthermore be chosen independently of each other. If (R_1, R_2) lies in region 3, the design criteria 2a) and 2b) have to be applied to the sum of the two codeword difference matrices $\mathbf{R}_3 = \mathbf{R}_1 + \mathbf{R}_2$ (joint design). Note, however, that the users will not cooperate in selecting their codewords. In the case of a general number of users, the design rule is to apply 2a) and 2b) to the sum of the codeword difference matrices corresponding to the subset of users leading to the dominant error event.

¹The proof consists of establishing lower and upper bounds on the right-hand side (RHS) of (1.6) and showing their asymptotic (in ρ) tightness.

²In the case where not all \mathbf{R}_k have full rank, the optimization in this step extends only over the \mathbf{R}_k with minimum rank.

³By effective channel we mean the physical channel in combination with the space-time/frequency code.

Low-SNR Design Criteria

In the low-SNR regime, using the approximation $e^{-x} \approx 1 - x$ on the LHS of the argument of $P(\cdot)$ in (1.4), we can state

Theorem 3. *For small ρ (keeping R_k fixed), the error probability P_{ek} ($k = 1, 2, 3$) satisfies⁴*

$$P_{ek} \lesssim \mathbb{P} \left(\sum_{n=0}^{N-1} \chi_n \lambda_n(\mathbf{R}_k) \leq \frac{4}{\rho} e^{NR_k^0} (1 - e^{-NR_k}) \right) \quad (1.7)$$

where the χ_n denote independent χ^2 -distributed random variables with $2M_R$ degrees of freedom each and $\lambda_n(\mathbf{R}_k)$ stands for the n th eigenvalue of

$$\mathbf{R}_k = \frac{1}{\widetilde{M}_k} \sum_{\substack{\mathbf{C}_k, \mathbf{E}_k \\ \mathbf{C}_k \neq \mathbf{E}_k}} \mathbf{G}(\mathbf{C}_k, \mathbf{E}_k) \mathbf{G}^H(\mathbf{C}_k, \mathbf{E}_k). \quad (1.8)$$

Noting that for small ρ the RHS of (1.7) is Schur-concave in the eigenvalues $\lambda_n(\mathbf{R}_k)$, it follows that in the low-SNR regime, optimum code design amounts to minimizing the rank of \mathbf{R}_k in (1.8), which implies that the rank of each term on the RHS of (1.8) should be minimized with all terms having the same range space. We note that this result cannot be obtained by specializing the classical code design criteria in [2, 3, 4] to the low-SNR case.

1.1.5 Numerical Example

In the following, we present a numerical example for the high-SNR regime, highlighting the importance of joint code designs. We consider a two-user system with $M_T = M_R = 2$, $N = 4$ and $L = 1$. If $x_1(i), x_2(i)$ for $i = 1, 2, 3, 4$ are the independently chosen QPSK data symbols of user 1 and 2, respectively, then the codeword matrices for user 1 take the form

$$\mathbf{C}_1 = \begin{bmatrix} x_1(1) & x_1(2) & x_1(3) & x_1(4) \\ -x_1^*(2) & x_1^*(1) & -x_1^*(4) & x_1^*(3) \end{bmatrix} \quad (1.9)$$

which is simply a concatenation of two Alamouti-type [15] codewords. Choosing \mathbf{C}_2 to be of the same form as \mathbf{C}_1 , both users' codes achieve maximum diversity order in single-user channels. However, such a design does not take the type-3 error events into account, since the minimum rank of $\overline{\mathbf{C}} - \overline{\mathbf{E}}$ (and hence of $\mathbf{R}_3 = \mathbf{R}_1 + \mathbf{R}_2$) is two only, e.g., there are codeword difference matrices that are of the form

$$\overline{\mathbf{C}} - \overline{\mathbf{E}} = \begin{bmatrix} \times & 0 & 0 & 0 \\ 0 & \times & 0 & 0 \\ \times & 0 & 0 & 0 \\ 0 & \times & 0 & 0 \end{bmatrix}$$

⁴Note that the inequality in (1.4) becomes approximate as a result of the small- x approximation of e^{-x} .

where \times denotes a nonzero entry. If instead, we use a joint design obtained by composing the codewords \mathbf{C}_2 as (obtained by swapping columns 2 and 3 in (1.9) and multiplying column 3 of the resulting matrix by $e^{-j\pi/8}$)

$$\mathbf{C}_2 = \begin{bmatrix} x_2(1) & x_2(3) & e^{-j\frac{\pi}{8}}x_2(2) & x_2(4) \\ -x_2^*(2) & -x_2^*(4) & e^{-j\frac{\pi}{8}}x_2^*(1) & x_2^*(3) \end{bmatrix}$$

while \mathbf{C}_1 remains unchanged, the resulting codeword difference matrices $\overline{\mathbf{C}} - \overline{\mathbf{E}}$ will have a minimum rank of three (as opposed to two in the original design), which results in a higher diversity order for the type-3 error events. Fig. 1.2 shows the corresponding error probabilities P_{e3} (obtained through Monte-Carlo simulations). Clearly, the joint design exhibits superior performance.

1.2 Outage Analysis of Ricean Fading MIMO Channels

1.2.1 Introduction

Analytical approaches for computing the performance limits of multiple-input multiple-output (MIMO) wireless channels commonly rely on the Rayleigh fading assumption [16, 17, 18]. In practice, however, the channel often exhibits a static component, especially in fixed wireless scenarios [1], which suggests a Ricean fading distribution. Despite their practical relevance, capacity results for Ricean MIMO channels remain scarce. Capacity bounds for spatially correlated Ricean MIMO channels can be found in [19]. Properties of the capacity achieving input distribution have been reported in [20, 21]. Results on the eigenvalue distribution of Ricean MIMO channels can be found in [22], and an asymptotic (in the number of antennas) capacity analysis has been carried out in [23]. Most of the results available in the literature are based on the classical i.i.d. complex Gaussian assumption for the random component of the channel matrix. For orthogonal space-time block codes, it was demonstrated in [24] that a more general Ricean MIMO channel model allowing for correlated entries in the random component of the channel matrix gives rise to the notion of a *critical rate*. For data rates below the critical rate, the fading channel behaves like an additive white Gaussian noise (AWGN) channel and communication with zero outage is possible. Above the critical rate, the channel exhibits Ricean fading behavior. A nonzero critical rate is possible only if the correlation matrix \mathbf{R} of the random component of the channel matrix is rank-deficient and the Ricean component spans dimensions in the null space of \mathbf{R} . The analysis in [24] only covers the case of Ricean MIMO channels in conjunction with orthogonal space-time block codes, which turn the MIMO channel into an effective single-input single-output channel.

Contributions: The main theme of the present paper is to establish the notion of a critical rate for the general MIMO case. Our detailed contributions can be summarized as follows:

- We compute the critical rate for general Ricean MIMO channels as a function of the channel statistics.

- We provide a complete characterization of the optimum diversity-multiplexing (DM) tradeoff for Ricean MIMO channels taking into account the existence of the critical rate, thereby establishing the notion of a critical multiplexing gain.

Notation: The superscripts T , H and $*$ stand for transposition, conjugate transposition and conjugation, respectively. \mathbf{I}_N is the $N \times N$ identity matrix, $\mathbf{0}$ is the all-zeros matrix of appropriate size, and $\|\mathbf{x}\|$ stands for the Euclidean norm of the vector \mathbf{x} . $\text{diag}_{n=1}^N\{a_n\}$ is the $N \times N$ diagonal matrix with diagonal elements a_n . For an $M \times N$ matrix $\mathbf{A} = [\mathbf{a}_1 \ \mathbf{a}_2 \ \cdots \ \mathbf{a}_N]$, we define $\text{vec}\{\mathbf{A}\} = [\mathbf{a}_1^T \ \mathbf{a}_2^T \ \cdots \ \mathbf{a}_N^T]^T$ and $\|\mathbf{A}\|_F$ is the Frobenius norm of \mathbf{A} . $\mathcal{E}[\cdot]$ denotes the expectation operator. \mathbb{R}_0^+ stands for the set of all nonnegative real numbers. A multivariate, circularly symmetric, zero-mean, complex Gaussian random vector is a random vector $\mathbf{z} = \mathbf{x} + j\mathbf{y} \sim \mathcal{CN}(\mathbf{0}, \mathbf{\Sigma})$, where the real-valued random vectors \mathbf{x} and \mathbf{y} are jointly Gaussian, $\mathcal{E}[\mathbf{z}] = \mathbf{0}$, $\mathcal{E}[\mathbf{z}\mathbf{z}^H] = \mathbf{\Sigma}$, and $\mathcal{E}[\mathbf{z}\mathbf{z}^T] = \mathbf{0}$. $f(x)$ and $g(x)$ are said to be exponentially equal, denoted by $f(x) \doteq g(x)$, if $\lim_{x \rightarrow \infty} \frac{\log f(x)}{\log x} = \lim_{x \rightarrow \infty} \frac{\log g(x)}{\log x}$. Exponential inequality, denoted by $\stackrel{\leq}{\sim}$ and $\stackrel{\geq}{\sim}$, is defined analogously. Logarithms are to the base e unless stated otherwise.

1.2.2 System Model

We consider a point-to-point frequency-flat fading MIMO channel with M_T transmit and M_R receive antennas. The corresponding channel matrix is given by

$$\mathbf{H} = \bar{\mathbf{H}} + \mathbf{R}^{1/2}\mathbf{H}_w$$

where $\bar{\mathbf{H}} = \mathcal{E}[\mathbf{H}]$ represents the fixed (static) channel component and $\mathbf{R}^{1/2}\mathbf{H}_w$ with $\text{vec}\{\mathbf{H}_w\} \sim \mathcal{CN}(\mathbf{0}, \mathbf{I}_{M_R M_T})$ denotes the zero-mean random channel component. The $M_R \times M_R$ receive correlation matrix \mathbf{R} is of rank r . The transmit antennas are assumed to fade in an uncorrelated fashion. The input-output relation is given by

$$\mathbf{y} = \sqrt{\rho}\mathbf{H}\mathbf{c} + \mathbf{z}$$

where ρ stands for the signal-to-noise ratio (SNR), $\mathbf{c} \sim \mathcal{CN}(\mathbf{0}, \frac{1}{M_T}\mathbf{I}_{M_T})$ denotes the M_T -dimensional transmit signal vector, and $\mathbf{z} \sim \mathcal{CN}(\mathbf{0}, \mathbf{I}_{M_R})$ represents the additive noise vector. Finally, throughout the paper, the receiver is assumed to have perfect knowledge of the channel, whereas the transmitter does not have any channel state information (CSI), but is aware of the channel statistics.

1.2.3 The Notion of a ‘‘Critical Rate’’

Our first main result, summarized in Theorem 4 below, provides an expression for the critical rate in the general MIMO case and shows that a geometrical interpretation, similar to the one provided in [24], can be given.

Theorem 4. *The mutual information of the Ricean MIMO channel with channel matrix $\mathbf{H} = \bar{\mathbf{H}} + \mathbf{R}^{1/2}\mathbf{H}_w$ can be decomposed as*

$$I = \log \det \left(\mathbf{I}_{M_T} + \frac{\rho}{M_T} \mathbf{B}^H \mathbf{B} \right) + I_f$$

where I_f is a nonnegative random variable and $\mathbf{B} = \mathbf{U}_\perp^H \bar{\mathbf{H}}$ with \mathbf{U}_\perp containing the eigenvectors corresponding to the zero eigenvalues of \mathbf{R} .

Proof. Based on the eigendecomposition $\mathbf{R} = \mathbf{U}\mathbf{\Lambda}\mathbf{U}^H$, we define $\mathbf{U} = [\mathbf{U}_\parallel \ \mathbf{U}_\perp]$, where \mathbf{U}_\parallel and \mathbf{U}_\perp contain the eigenvectors corresponding to the nonzero and zero eigenvalues, respectively, of \mathbf{R} . Analogously, we define

$$\mathbf{\Lambda} = \begin{bmatrix} \mathbf{\Lambda}_+ & \\ & \mathbf{0} \end{bmatrix}$$

so that $\mathbf{R} = \mathbf{U}_\parallel \mathbf{\Lambda}_+ \mathbf{U}_\parallel^H$. Since \mathbf{U} is a unitary $M_R \times M_R$ matrix, we can write

$$I = \log \det \left(\mathbf{I}_{M_R} + \frac{\rho}{M_T} \mathbf{U}^H \mathbf{H} \mathbf{H}^H \mathbf{U} \right). \quad (1.10)$$

Letting $\tilde{\mathbf{H}}_w$ be an $r \times M_T$ matrix such that $\text{vec}\{\tilde{\mathbf{H}}_w\} \sim \mathcal{CN}(\mathbf{0}, \mathbf{I}_{rM_T})$ yields

$$\begin{aligned} \mathbf{U}^H \mathbf{H} &\sim \mathbf{U}^H \bar{\mathbf{H}} + \mathbf{U}^H \mathbf{U}_\parallel \mathbf{\Lambda}_+^{1/2} \tilde{\mathbf{H}}_w \\ &= \begin{bmatrix} \mathbf{U}_\parallel^H \bar{\mathbf{H}} \\ \mathbf{U}_\perp^H \bar{\mathbf{H}} \end{bmatrix} + \begin{bmatrix} \mathbf{\Lambda}_+^{1/2} \tilde{\mathbf{H}}_w \\ \mathbf{0} \end{bmatrix} \end{aligned}$$

and hence

$$\mathbf{U}^H \mathbf{H} \mathbf{H}^H \mathbf{U} \sim \begin{bmatrix} \mathbf{A} \mathbf{A}^H & \mathbf{A} \mathbf{B}^H \\ \mathbf{B} \mathbf{A}^H & \mathbf{B} \mathbf{B}^H \end{bmatrix}$$

where $\mathbf{A} = \mathbf{U}_\parallel^H \bar{\mathbf{H}} + \mathbf{\Lambda}_+^{1/2} \tilde{\mathbf{H}}_w$ and $\mathbf{B} = \mathbf{U}_\perp^H \bar{\mathbf{H}}$. Therefore, the mutual information in (1.10) can be expressed as

$$I = \log \det \left(\begin{bmatrix} \mathbf{I}_r + \frac{\rho}{M_T} \mathbf{A} \mathbf{A}^H & \frac{\rho}{M_T} \mathbf{A} \mathbf{B}^H \\ \frac{\rho}{M_T} \mathbf{B} \mathbf{A}^H & \mathbf{I}_{M_R-r} + \frac{\rho}{M_T} \mathbf{B} \mathbf{B}^H \end{bmatrix} \right).$$

Employing the Schur complement formula for determinants [25, Thm. 0.8.5], we get

$$I = \log \det \left(\mathbf{I}_{M_R-r} + \frac{\rho}{M_T} \mathbf{B} \mathbf{B}^H \right) + I_f \quad (1.11)$$

where

$$I_f = \log \det \left(\mathbf{I}_r + \frac{\rho}{M_T} \mathbf{A} \mathbf{A}^H - \frac{\rho^2}{M_T^2} \mathbf{A} \mathbf{B}^H \left(\mathbf{I}_{M_R-r} + \frac{\rho}{M_T} \mathbf{B} \mathbf{B}^H \right)^{-1} \mathbf{B} \mathbf{A}^H \right). \quad (1.12)$$

Applying $\det(\mathbf{I} + \mathbf{X}\mathbf{Y}) = \det(\mathbf{I} + \mathbf{Y}\mathbf{X})$ to the first term on the right-hand side (RHS) of (1.11) then yields the desired result. The expression for I_f in (1.12) can be simplified by using the matrix inversion lemma [25, Thm. 0.7.4] to obtain

$$I_f = \log \det \left(\mathbf{I}_r + \frac{\rho}{M_T} \mathbf{A} \left(\mathbf{I}_{M_T} + \frac{\rho}{M_T} \mathbf{B}^H \mathbf{B} \right)^{-1} \mathbf{A}^H \right).$$

Noting that the matrix $\mathbf{A} \left(\mathbf{I}_{M_T} + \frac{\rho}{M_T} \mathbf{B}^H \mathbf{B} \right)^{-1} \mathbf{A}^H$ is positive semidefinite, it follows that $I_f \geq 0$, which completes the proof.

With the outage probability at rate R defined as

$$P_e(R) = \mathbb{P}(I \leq R)$$

Theorem 4 implies $P_e(R) = 0$ for $R \leq R_{\text{crit}}$ where

$$R_{\text{crit}} = \log \det \left(\mathbf{I}_{M_T} + \frac{\rho}{M_T} \mathbf{B}^H \mathbf{B} \right). \quad (1.13)$$

Equivalently, this result says that for rates below the critical rate, communication with zero outage is possible, i.e., the fading channel behaves like an AWGN channel. We infer from (1.13) that the critical rate is the capacity of an effective AWGN channel with the $(M_R - r) \times M_T$ transfer matrix \mathbf{B} ; this effective AWGN channel is determined by the projection of the range space of $\overline{\mathbf{H}}$ onto the null space of \mathbf{R} . In other words, the effective MIMO channel with transfer matrix \mathbf{B} is spanned by those dimensions of $\overline{\mathbf{H}}$ that are not impaired by fading. The critical rate is equal to zero in the following cases: i) $\text{rank}\{\mathbf{R}\} = M_R$; ii) $\overline{\mathbf{H}} = \mathbf{0}$; iii) $\text{rank}\{\mathbf{R}\} < M_R$, $\overline{\mathbf{H}} \neq \mathbf{0}$, and $\mathbf{U}_\perp^H \overline{\mathbf{H}} = \mathbf{B} = \mathbf{0}$, i.e., $\overline{\mathbf{H}}$ lies completely in the range space of \mathbf{R} . Similar to [24], one can express the critical rate as a function of the principal angles [26] between the subspaces spanned by $\overline{\mathbf{H}}$ and by \mathbf{R} .

We conclude by noting that in the special case of a multiple-input single-output (MISO) channel where

$$I = \log \left(1 + \frac{\rho}{M_T} \|\mathbf{H}\|_F^2 \right)$$

the expression for the critical rate in (1.13) can be shown to reduce to the critical rate computed in [24].

1.2.4 Diversity-Multiplexing Tradeoff

In the following, we provide a complete characterization of the DM tradeoff [27] for Ricean MIMO channels. We shall see that the concept of a critical rate leads to the concept of a critical multiplexing gain.

Following [27], we define the diversity gain corresponding to a multiplexing gain of m as

$$d(m) = - \lim_{\rho \rightarrow \infty} \frac{\log \mathbb{P}(I \leq m \log \rho)}{\log \rho}.$$

The optimality of the i.i.d. Gaussian input distribution with respect to the DM tradeoff can be established pursuing the same line of reasoning as in [27].

Before tackling the computation of the DM tradeoff curve for the general Ricean MIMO channel, we need the following Lemma, which states that the presence of a nonzero mean channel component does not alter the DM tradeoff behavior as long as the random channel component is i.i.d. complex Gaussian.

Lemma 5. *The outage probability P_e of the $n \times k$ Ricean MIMO channel with channel matrix $\mathbf{H} = \overline{\mathbf{H}} + \mathbf{H}_w$, where \mathbf{H}_w is such that $\text{vec}\{\mathbf{H}_w\} \sim \mathcal{CN}(\mathbf{0}, \mathbf{I}_{nk})$, satisfies*

$$P_e \doteq \text{P} \left(\log \det \left(\mathbf{I}_n + \frac{\rho}{M_T} \mathbf{H}_w \mathbf{H}_w^H \right) \leq m \log \rho \right).$$

Proof. The key idea of the proof is to show that setting the mean component of any column vector \mathbf{h}_i ($i = 1, 2, \dots, k$) of $\mathbf{H} = [\mathbf{h}_1 \ \mathbf{h}_2 \ \dots \ \mathbf{h}_k]$ to $\mathbf{0}$ preserves the exponential order of P_e . This result can be applied successively to all columns, thereby establishing the proof of the general statement. Without loss of generality, we provide the proof for the first column \mathbf{h}_1 .

The mutual information of the Ricean MIMO channel with channel matrix \mathbf{H} can be written as

$$I = \log \det \left(\mathbf{I}_n + \frac{\rho}{M_T} \sum_{i=1}^k \mathbf{h}_i \mathbf{h}_i^H \right). \quad (1.14)$$

Defining the nonsingular (w. p. 1) $n \times n$ matrix $\mathbf{M} = \mathbf{I}_n + \frac{\rho}{M_T} \sum_{i=2}^k \mathbf{h}_i \mathbf{h}_i^H$ allows to rewrite (1.14) as

$$I = \log \det(\mathbf{M}) + \log \left(1 + \frac{\rho}{M_T} \mathbf{h}_1^H \mathbf{M}^{-1} \mathbf{h}_1 \right).$$

Inspired by the fact that the matrix \mathbf{M} depends only on the random vectors $\mathbf{h}_2, \mathbf{h}_3, \dots, \mathbf{h}_k$, we express the outage probability P_e in terms of a conditional probability according to

$$\begin{aligned} P_e &= \mathcal{E}_{\mathbf{h}_2, \mathbf{h}_3, \dots, \mathbf{h}_k} \left[\text{P} \left(I \leq m \log \rho \mid \mathbf{h}_2, \mathbf{h}_3, \dots, \mathbf{h}_k \right) \right] \\ &= \mathcal{E}_{\mathbf{h}_2, \mathbf{h}_3, \dots, \mathbf{h}_k} \left[\text{P} \left(\mathbf{h}_1^H \mathbf{M}^{-1} \mathbf{h}_1 \leq \frac{M_T}{\rho} (\rho^m \det(\mathbf{M}^{-1}) - 1) \mid \mathbf{h}_2, \mathbf{h}_3, \dots, \mathbf{h}_k \right) \right]. \end{aligned}$$

Noting that the elements of the vector \mathbf{h}_1 are independent complex Gaussian random variables with unit variance, but possibly different means, it follows from [28, Eq. (3.1a.4)] that (conditioned on $\mathbf{h}_2, \mathbf{h}_3, \dots, \mathbf{h}_k$) we have $\mathbf{h}_1^H \mathbf{M}^{-1} \mathbf{h}_1 = \sum_{i=1}^n \lambda_{M,i}^{-1} \chi_i$, where the χ_i ($i = 1, 2, \dots, n$) are independent noncentral χ^2 -distributed random variables with noncentrality parameters $\bar{\chi}_i$ and two degrees of freedom each; $\lambda_{M,i}^{-1} > 0$ ($i = 1, 2, \dots, n$) denotes the i th eigenvalue of \mathbf{M}^{-1} .

Defining the set $\mathcal{A}_{\mathbf{h}}$ conditioned on $\mathbf{h}_2, \mathbf{h}_3, \dots, \mathbf{h}_k$ as

$$\mathcal{A}_{\mathbf{h}} = \left\{ \mathbf{v} \in (\mathbb{R}_0^+)^n : \sum_{i=1}^n \lambda_{M,i}^{-1} v_i \leq \frac{M_T}{\rho} (\rho^m \det(\mathbf{M}^{-1}) - 1) \right\}$$

enables us to write

$$P_e = \mathcal{E}_{\mathbf{h}_2, \mathbf{h}_3, \dots, \mathbf{h}_k} \left[\int_{\mathbf{v} \in \mathcal{A}_{\mathbf{h}}} p_{\chi_1, \chi_2, \dots, \chi_n}(\mathbf{v}) d\mathbf{v} \right]$$

where $p_{\chi_1, \chi_2, \dots, \chi_n}(\mathbf{v})$ follows from [29, p. 76] as

$$p_{\chi_1, \chi_2, \dots, \chi_n}(\mathbf{v}) = \prod_{i=1}^n e^{-(\bar{\chi}_i + v_i)} \left(\sum_{l=0}^{\infty} \frac{(4v_i \bar{\chi}_i)^l}{(l!)^2} \right). \quad (1.15)$$

Next, in order to reveal the exponential order behavior of P_e , we set $v_i = \rho^{-\alpha_i}$ ($i = 1, 2, \dots, n$) so that the term for $l = 0$ in the power series expansion of (1.15) can be seen to dominate the error probability and therefore

$$P_e \doteq \mathcal{E}_{\mathbf{h}_2, \mathbf{h}_3, \dots, \mathbf{h}_k} \left[\int_{\boldsymbol{\alpha}: \rho^{-\boldsymbol{\alpha}} \in \mathcal{A}_{\mathbf{h}}} (\log \rho)^n \prod_{i=1}^n e^{-\bar{\chi}_i} e^{-\rho^{-\alpha_i}} \rho^{-\alpha_i} d\boldsymbol{\alpha} \right]$$

where the notation $\boldsymbol{\alpha} : \rho^{-\boldsymbol{\alpha}} \in \mathcal{A}_{\mathbf{h}}$ means $(\alpha_1, \alpha_2, \dots, \alpha_n) : [\rho^{-\alpha_1} \rho^{-\alpha_2} \dots \rho^{-\alpha_n}] \in \mathcal{A}_{\mathbf{h}}$.

We note that $\prod_{i=1}^n e^{-\bar{\chi}_i} = e^{-\|\mathcal{E}[\mathbf{h}_1]\|^2}$ reduces to a constant factor which does not affect the exponential order of P_e . Furthermore, the factor $(\log \rho)^n$ has no impact on the exponential order of P_e either, since it grows only logarithmically in ρ so that

$$P_e \doteq \mathcal{E}_{\mathbf{h}_2, \mathbf{h}_3, \dots, \mathbf{h}_k} \left[\int_{\boldsymbol{\alpha}: \rho^{-\boldsymbol{\alpha}} \in \mathcal{A}_{\mathbf{h}}} \prod_{i=1}^n e^{-\rho^{-\alpha_i}} \rho^{-\alpha_i} d\boldsymbol{\alpha} \right]. \quad (1.16)$$

Next, we note that following the same steps as above for $\mathcal{E}[\mathbf{h}_1] = 0$ would lead to

$$p_{\chi_1, \chi_2, \dots, \chi_n}(\mathbf{v}) = \prod_{i=1}^n e^{-v_i}$$

which upon applying the transformation $v_i = \rho^{-\alpha_i}$ ($i = 1, 2, \dots, n$) results in P_e satisfying (1.16). This shows that the presence of a nonzero mean does not affect the exponential behavior of P_e . As mentioned at the outset, successively applying this result to all columns of \mathbf{H} completes the proof.

Since $R_{\text{crit}} \doteq m_{\text{crit}} \log \rho$ with $m_{\text{crit}} = \text{rank}\{\mathbf{B}\}$, it follows by inspection that $d(m) = \infty$ for $m \leq m_{\text{crit}}$. We note that

$$\begin{aligned} P_e &= \text{P}(I_f + R_{\text{crit}} \leq m \log \rho) \\ &\doteq \text{P}(I_f + m_{\text{crit}} \log \rho \leq m \log \rho) \\ &= \text{P}(I_f \leq \Delta m \log \rho) \end{aligned} \quad (1.17)$$

where $\Delta m = m - m_{\text{crit}}$. It remains to determine $d(m)$ for $m > m_{\text{crit}}$, which, as a consequence of (1.17), can be done by characterizing the exponential behavior of

$$P_f = \text{P}(I_f \leq \Delta m \log \rho).$$

This will be accomplished by showing that P_f is exponentially equal to the outage probability of a zero-mean i.i.d. Gaussian MIMO channel with appropriate dimensions, for which the DM tradeoff curve has already been characterized in [27].

Lemma 6. *The probability P_f satisfies*

$$P_f \doteq \mathbb{P} \left(\log \det \left(\mathbf{I}_{M_T-b} + \frac{\rho}{M_T} \widehat{\mathbf{A}}^H \widehat{\mathbf{A}} \right) \leq \Delta m \log \rho \right)$$

where $b = \text{rank}\{\mathbf{B}\}$, $\widehat{\mathbf{A}} = \mathbf{\Lambda}_+^{-1/2} \mathbf{U}_{\parallel}^H \overline{\mathbf{H}} \mathbf{V}_{\perp} + \widehat{\mathbf{H}}_w$ with $\text{vec}\{\widehat{\mathbf{H}}_w\} \sim \mathcal{CN}(\mathbf{0}, \mathbf{I}_{r(M_T-b)})$ and \mathbf{V}_{\perp} denotes the $M_T \times (M_T - b)$ matrix containing the eigenvectors of $\mathbf{B}^H \mathbf{B} = \mathbf{V} \mathbf{\Lambda}_B \mathbf{V}^H$ corresponding to zero eigenvalues.

Proof. The proof idea is to establish an upper and a lower bound on P_f , which are exponentially equal. We start by rewriting I_f as

$$I_f = \log \det \left(\mathbf{I}_r + \mathbf{A} \mathbf{V} \text{diag}_{i=1}^{M_T} \left\{ \frac{\rho}{M_T + \rho \lambda_{B,i}} \right\} \mathbf{V}^H \mathbf{A}^H \right)$$

where $\lambda_{B,i} = \lambda_i(\mathbf{B}^H \mathbf{B})$ ($i = 1, 2, \dots, M_T$). Next, we split up the $M_T \times M_T$ matrix \mathbf{V} according to

$$\mathbf{V} = [\mathbf{V}_{\parallel} \quad \mathbf{V}_{\perp}]$$

where \mathbf{V}_{\parallel} denotes the matrix containing the eigenvectors of $\mathbf{B}^H \mathbf{B}$ corresponding to the b nonzero eigenvalues. With the above definitions, we can write

$$I_f = \log \det \left(\mathbf{I}_r + \frac{\rho}{M_T} \mathbf{A} \mathbf{V}_{\perp} \mathbf{V}_{\perp}^H \mathbf{A}^H + \mathbf{A} \mathbf{V}_{\parallel} \text{diag}_{i=1}^b \left\{ \frac{\rho}{M_T + \rho \lambda_{B,i}} \right\} \mathbf{V}_{\parallel}^H \mathbf{A}^H \right).$$

Since both $\mathbf{A} \mathbf{V}_{\perp} \mathbf{V}_{\perp}^H \mathbf{A}^H$ and $\mathbf{A} \mathbf{V}_{\parallel} \text{diag}_{i=1}^b \{\rho / (M_T + \rho \lambda_{B,i})\} \mathbf{V}_{\parallel}^H \mathbf{A}^H$ are positive semidefinite, we can invoke a Theorem by Weyl [25, Thm. 4.3.1] to lower-bound I_f according to

$$I_f \geq \log \det \left(\mathbf{I}_r + \frac{\rho}{M_T} \mathbf{A} \mathbf{V}_{\perp} \mathbf{V}_{\perp}^H \mathbf{A}^H \right). \quad (1.18)$$

On the other hand, I_f can be upper-bounded using $\frac{\rho}{M_T + \rho \lambda_{B,i}} \leq \frac{1}{\lambda_{B,i}}$ and resorting again to the result by Weyl [25, Thm. 4.3.1] to obtain

$$I_f \leq \log \det \left(\mathbf{I}_r + \frac{\rho}{M_T} \mathbf{A} \mathbf{V}_{\perp} \mathbf{V}_{\perp}^H \mathbf{A}^H + \mathbf{A} \mathbf{V}_{\parallel} \text{diag}_{i=1}^b \{\lambda_{B,i}^{-1}\} \mathbf{V}_{\parallel}^H \mathbf{A}^H \right). \quad (1.19)$$

The last term inside the argument of the RHS of (1.19) is independent of ρ . Therefore, in the $\rho \rightarrow \infty$ limit, the upper and lower bounds (1.18) and (1.19) coincide, which yields

$$P_f \doteq \mathbb{P} \left(\log \det \left(\mathbf{I}_r + \frac{\rho}{M_T} \mathbf{A} \mathbf{V}_{\perp} \mathbf{V}_{\perp}^H \mathbf{A}^H \right) \leq \Delta m \log \rho \right).$$

The matrix product $\mathbf{A}\mathbf{V}_\perp$ can be expressed as

$$\mathbf{A}\mathbf{V}_\perp \sim \mathbf{U}_\parallel^H \overline{\mathbf{H}} \mathbf{V}_\perp + \mathbf{\Lambda}_+^{1/2} \widehat{\mathbf{H}}_w$$

where we exploited the fact that $\widetilde{\mathbf{H}}_w \mathbf{V}_\perp \sim \widehat{\mathbf{H}}_w$ with $\text{vec}\{\widehat{\mathbf{H}}_w\} \sim \mathcal{CN}(\mathbf{0}, \mathbf{I}_{r(M_T-b)})$ due to the orthonormality of the columns of \mathbf{V}_\perp . Defining

$$\widehat{\mathbf{A}} = \mathbf{\Lambda}_+^{-1/2} \mathbf{U}_\parallel^H \overline{\mathbf{H}} \mathbf{V}_\perp + \widehat{\mathbf{H}}_w$$

and employing the relation $\log \det(\mathbf{I} + \mathbf{X}\mathbf{Y}) = \log \det(\mathbf{I} + \mathbf{Y}\mathbf{X})$ yields

$$P_f \doteq \mathbb{P} \left(\log \det \left(\mathbf{I}_{M_T-b} + \frac{\rho}{M_T} \widehat{\mathbf{A}}^H \mathbf{\Lambda}_+ \widehat{\mathbf{A}} \right) \leq \Delta m \log \rho \right).$$

Note that the $r \times r$ real-valued diagonal matrix $\mathbf{\Lambda}_+$ is nonsingular. We denote the smallest diagonal element of $\mathbf{\Lambda}_+$ by λ_{\min} and the largest by λ_{\max} . Due to the concavity of $\log \det(\mathbf{I} + \mathbf{P})$ over the convex set of positive definite Hermitian matrices \mathbf{P} [25, Thm. 7.6.7], we obtain the following bounds

$$\begin{aligned} P_f &\leq \mathbb{P} \left(\log \det \left(\mathbf{I}_{M_T-b} + \frac{\lambda_{\min} \rho}{M_T} \widehat{\mathbf{A}}^H \widehat{\mathbf{A}} \right) \leq \Delta m \log \rho \right) \\ P_f &\geq \mathbb{P} \left(\log \det \left(\mathbf{I}_{M_T-b} + \frac{\lambda_{\max} \rho}{M_T} \widehat{\mathbf{A}}^H \widehat{\mathbf{A}} \right) \leq \Delta m \log \rho \right). \end{aligned}$$

Since scaling (by the constants λ_{\min} and λ_{\max}) of the SNR does not have an impact on the exponential (in ρ) behavior of P_f , we can conclude that

$$P_f \doteq \mathbb{P} \left(\log \det \left(\mathbf{I}_{M_T-b} + \frac{\rho}{M_T} \widehat{\mathbf{A}}^H \widehat{\mathbf{A}} \right) \leq \Delta m \log \rho \right)$$

which proves the lemma.

The findings of Lemma 6 show that for $m > m_{\text{crit}}$ the DM tradeoff is equivalent to that of an $r \times (M_T - m_{\text{crit}})$ -dimensional Ricean MIMO channel, whose random channel component consists of i.i.d. complex Gaussian elements. By combining Lemma 5 and Lemma 6, we have finally proven the following result.

Theorem 7. *The DM tradeoff curve for the general Ricean MIMO channel $\mathbf{H} = \overline{\mathbf{H}} + \mathbf{R}^{1/2} \mathbf{H}_w$ with the rank- m_{crit} matrix $\mathbf{B} = \mathbf{U}_\perp^H \overline{\mathbf{H}}$ and $m_{\text{max}} = \min\{M_T, r + m_{\text{crit}}\}$ is given by the piecewise-linear function connecting the points $(m, d(m))$, $m = 0, 1, \dots, m_{\text{max}}$, where*

$$d(m) = \begin{cases} \infty, & m \leq m_{\text{crit}} \\ (r + m_{\text{crit}} - m)(M_T - m), & m_{\text{crit}} < m \leq m_{\text{max}}. \end{cases}$$

The DM tradeoff curve given by Theorem 7 essentially consists of two parts. For multiplexing gains up to the critical multiplexing gain $m_{\text{crit}} = \text{rank}\{\mathbf{B}\}$, the maximum achievable diversity order is infinity, since the channel behaves like an AWGN channel. For multiplexing gains above m_{crit} , the tradeoff curve equals that of an $r \times (M_T - m_{\text{crit}})$

Rayleigh fading MIMO channel. Note that for full-rank \mathbf{R} , i.e., $\text{rank}\{\mathbf{R}\} = M_R$, we have $m_{\text{crit}} = 0$ and the tradeoff curve in Theorem 7 is simply that of an $M_R \times M_T$ Rayleigh fading MIMO channel.

Numerical example: An example of a DM tradeoff curve for a Ricean MIMO channel with $M_R = M_T = 4$ is depicted in Fig. 1.3. We assumed $r = \text{rank}\{\mathbf{R}\} = 2$ and $\text{rank}\{\overline{\mathbf{H}}\} = 2$. Furthermore, the matrices \mathbf{R} and $\overline{\mathbf{H}}$ are chosen such that $m_{\text{crit}} = \text{rank}\{\mathbf{B}\} = 1$. Consequently, for $m \leq 1$, the channel behaves like an AWGN channel.

1.3 Concluding Remarks

We found space-time/frequency code design criteria for fading multiantenna MACs with perfect CSI at the receiver, using the concept of dominant error event regions first introduced in [8]. The essence of our design criteria is to recognize that, depending on the transmission rate tuple, joint code designs may or may not be necessary. It was shown that joint designs essentially require applying the classical design criteria [2, 3, 4] to a sum of codeword difference matrices, with the specific sum depending on the subset of users leading to the dominant error event for the given transmission rate tuple. Systematic joint code designs constitute an interesting area of research. Finally, we note that as a side result of our analysis we showed that the classical (based on pairwise error probability) code design criteria are recovered from a criterion that essentially aims at minimizing the probability of encountering a bad effective channel realization.

For the case of general Ricean fading MIMO channels, which exhibit an arbitrary mean channel component and a correlated random channel component, we analyzed the outage probability and the diversity-multiplexing tradeoff. Our results gave rise to the notion of critical rate, i.e., the maximum rate, below which transmission at zero outage probability is possible. The concept of critical rate turned out to play an important role in the characterization of the diversity-multiplexing tradeoff curve, as it essentially divides the range of multiplexing gains into two regimes: for multiplexing gains up to the multiplexing gain of the critical rate, the channel behaves like an AWGN channel, whereas for higher multiplexing gains, the tradeoff curve is equal to that of a Rayleigh fading MIMO channel with appropriate dimensions.

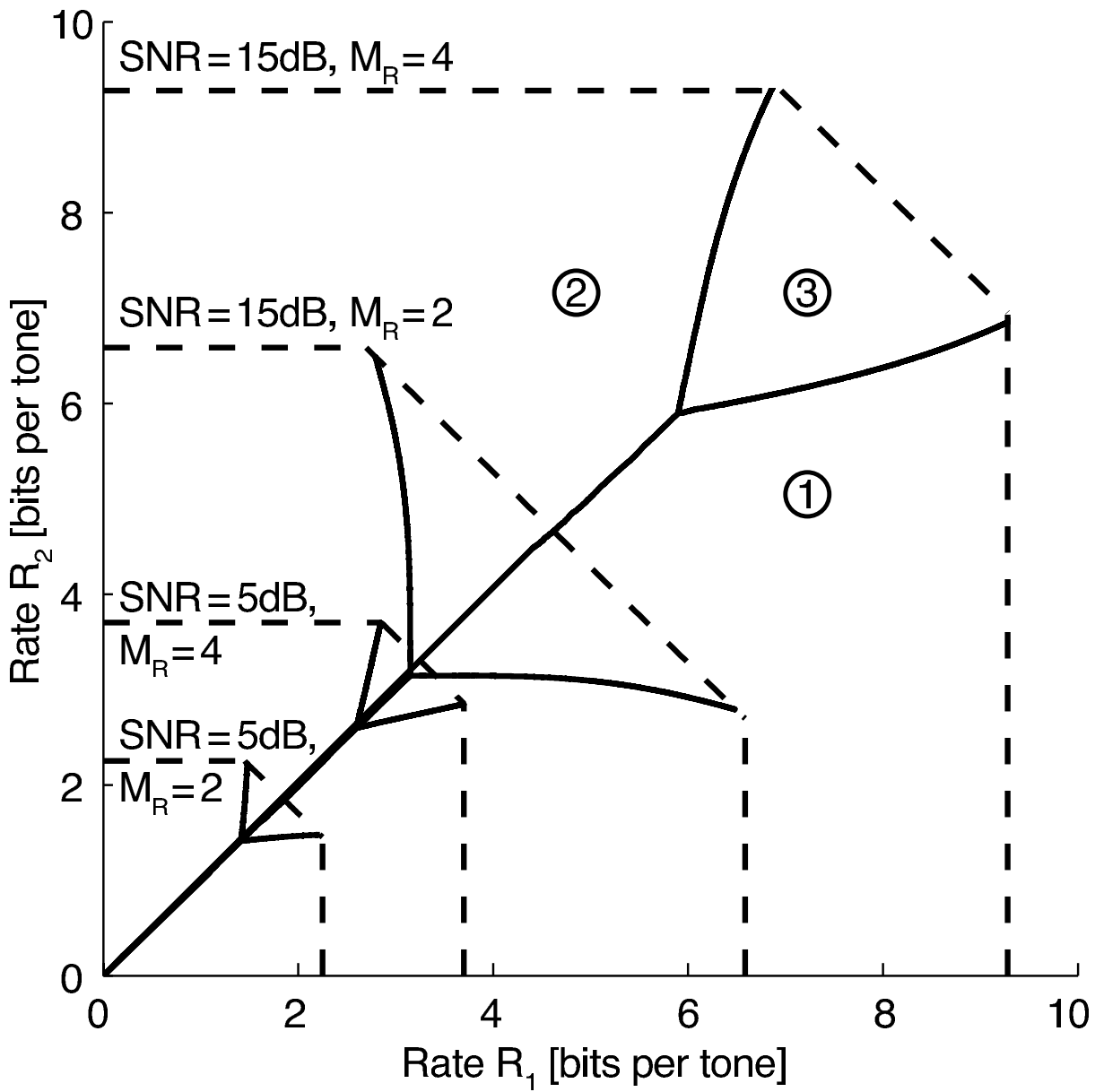


Figure 1.1: Dominant error event regions for the two-user MAC with $M_T = 2$ and $L = 1$. Dashed lines represent the ergodic capacity regions.

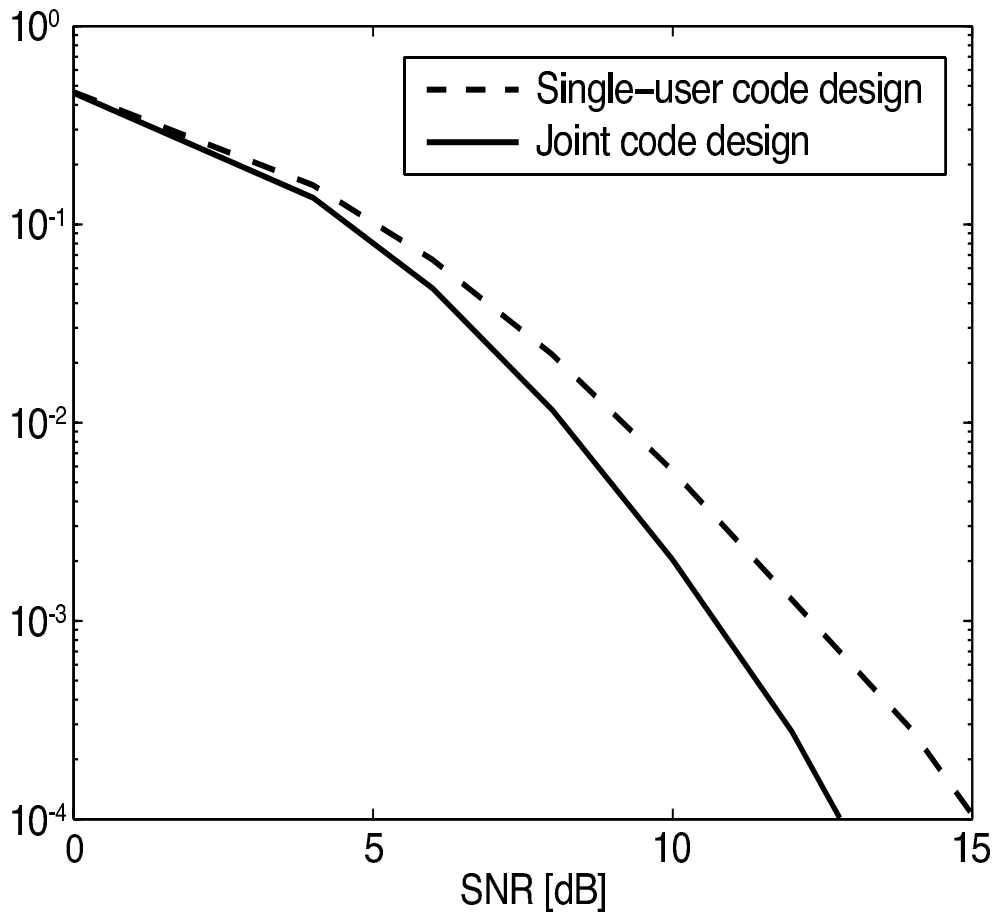


Figure 1.2: P_{e3} for single-user and joint code design as a function of SNR.

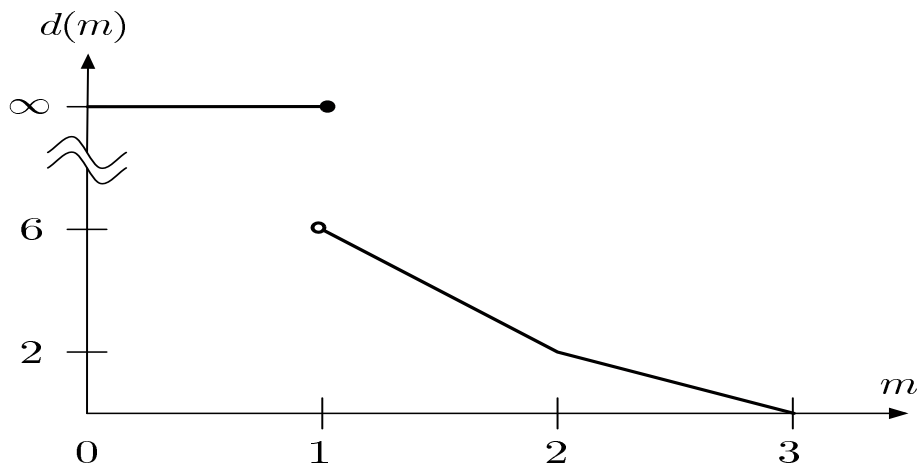


Figure 1.3: Diversity-multiplexing tradeoff curve for a Ricean MIMO channel with $M_R = M_T = 4$, $r = 2$ and $m_{\text{crit}} = 1$.

Chapter 2

MU-MIMO Downlink Space-Time Block Coded Transmission Scheme

2.1 Introduction

Space-time coding was proposed in [2] by combining channel coding and transmit diversity techniques in order to achieve diversity and coding gains. In the coherent scenario, where the channel state information (CSI) is available at the receiver, the design criteria for full diversity space-time codes in quasi-static fading channels were developed [2]. Space-time block codes (STBCs) attract a lot interests due to the low complexity of linear decoding, full diversity gain, and high transmission rates with low delay.

Orthogonal STBCs in [15, 30] and diagonal algebraic space-time (DAST) block codes in [31, 32] were proposed to achieve full diversity with a low complexity receiver. However, these codes do not achieve all the potential full transmission rates.

In [33], threaded algebraic space-time (TAST) block codes were proposed for arbitrary numbers of transmit and receive antennas. In [34], full rate and full rank linear dispersion STBCs were designed using cyclic division algebra.

However, the minimum determinants of the codeword difference matrix for the above constructions vanish for increasing size of the signal constellation. In [35, 36, 37], full rate and full diversity codes, named Perfect STBCs, with non-vanishing minimum determinants were proposed.

In the downlink of a multiple-input multiple-output (MIMO) multiuser system, a base station simultaneously transmits signals for many different users. Multiple antennas at both transmitters and receivers ensure high data rates, which are required in the next generation wireless communication systems. Hence it is natural to combine STBCs with downlink transmission schemes for a MIMO multiuser system. Recent work in [41] uses orthogonal STBCs in the downlink of a Direct Sequence Code Division Multiple Access (DS-CDMA) system, where the multiple-input single-output (MISO) case was considered.

In our paper, we consider CDMA as a multiplexing scheme. We show how to use TAST codes and perfect STBCs in the downlink of a MIMO multiuser system. Different orthogonal spreading matrices are used to separate the data streams of multiple users. At the receiver of each user, after despreading the received signal sequence, the maximum likelihood decoding is obtained by a lattice decoder. The performance of the downlink

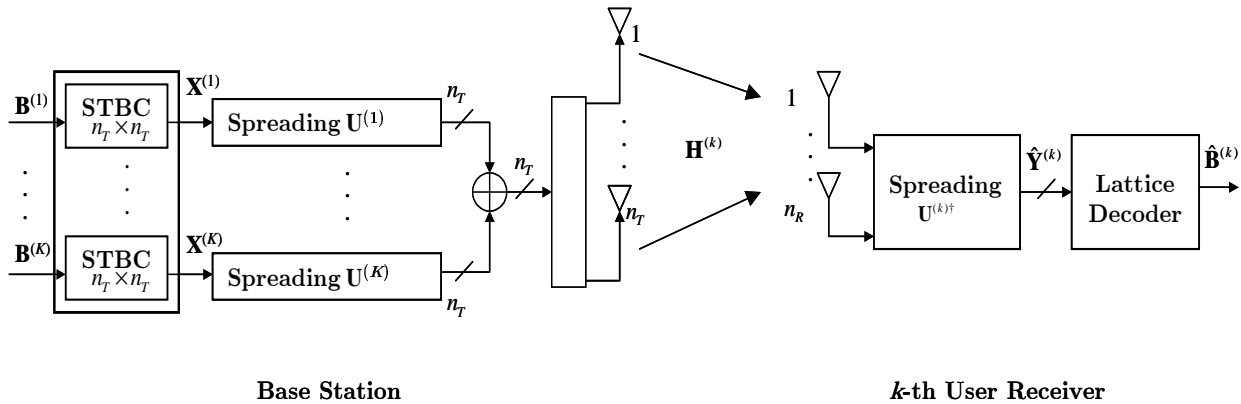


Figure 2.1: A MIMO Multiuser System

system is evaluated by simulation in terms of block error rate (BLER). Due to multipath propagation, different time delayed versions of the transmitted signal may result in multiple access interference (MAI). The impact of MAI on the system performance is also analyzed by simulation.

The rest of the paper is organized as follows. Section II introduces the system model. Section III presents how to apply TAST block codes and perfect STBCs to the downlink of MIMO multiuser systems. In Section IV, lattice decoding for this space-time block coded MIMO multiuser system is shown. Section V shows simulation results. Finally, conclusions are drawn in Section VI.

2.2 System Model

The following notations are used in the paper: T denotes transpose and \dagger denotes transpose conjugate. Let \mathbb{Z} , \mathbb{Q} , \mathbb{C} and $\mathbb{Z}[j]$ denote the ring of rational integers, the field of rational numbers, the field of complex numbers, and the ring of Gaussian integers, where $j^2 = -1$. Let \mathcal{S} and \mathcal{S}^2 denote PAM and QAM constellation sets, respectively. Let $\mathbb{Q}(\theta)$ denote an algebraic number field generated by the primitive element θ . The $m \times m$ dimensional identity matrix is denoted by \mathbf{I}_m . The matrix $\mathbf{1}_m$ is defined as an all ones $m \times m$ matrix. Given a m dimension vector \mathbf{v} , $\mathbf{V} = \text{diag}(\mathbf{v})$ is the $m \times m$ diagonal matrix with $\mathbf{V}_{i,i} = v_i$ and $\mathbf{V}_{i,k} = 0$ for all $i, k = 1, \dots, m$, and $i \neq k$.

We consider the downlink of a K user MIMO multiuser system, as shown in Fig. 1. We assume that the base station has n_T transmit antennas, where $n_T = \sum_{k=1}^K n_R^{(k)}$ and $n_R^{(k)}$ denotes the number of receive antennas for k -th user. This enables to support terminals with different receiver complexity.

Since the encoder and decoder structures for any user are similar, we only consider the general code construction and lattice decoding for an arbitrary k -th user. The superscript k is thus omitted for brevity.

For any k -th user, the base station transmits the $n_T \times n_R$ QAM information symbol

matrix

$$\begin{aligned} \mathbf{B} &= [\mathbf{b}_1 \ \mathbf{b}_2 \ \cdots \ \mathbf{b}_{n_R}] \\ &= \begin{bmatrix} b_{1,1} & b_{1,2} & \cdots & b_{1,n_R} \\ \vdots & \vdots & \ddots & \vdots \\ b_{n_T,1} & b_{n_T,2} & \cdots & b_{n_T,n_R} \end{bmatrix} \end{aligned} \quad (2.1)$$

where $b_{i,l} \in \mathbb{Z}[j]$, $i = 1, \dots, n_T$, $l = 1, \dots, n_R$.

In this paper, we consider square linear dispersion STBCs [36,37] with full rate and full diversity. The QAM information symbols are encoded by such STBCs into an $n_T \times n_T$ codeword matrix $\mathbf{X} = \{x_{i,l}\} \in \mathbb{C}$, $i, l = 1, \dots, n_T$. The codeword matrices for each user are separated by orthogonal spreading matrices. Let $\mathbf{U} \in \mathbb{C}^{n_T \times K n_T}$ be the orthogonal spreading matrix for user k and $\mathbf{U}^{(l)} \in \mathbb{C}^{n_T \times K n_T}$ be the one for another user l , where $l \neq k$. We have

$$\mathbf{U}\mathbf{U}^\dagger = \mathbf{I}_{n_T} \quad \mathbf{U}^{(l)}\mathbf{U}^\dagger = 0,$$

The orthogonal signature matrices can be chosen, for example, as submatrices of a discrete Fourier transform (DFT) matrix or Hadamard matrix.

We assume that perfect CSI is known at the receiver of each user. The k -th user receives the signal matrix $\mathbf{Y} \in \mathbb{C}^{n_R \times K n_T}$, which is given by

$$\mathbf{Y} = \mathbf{H}\mathbf{X}\mathbf{U} + \mathbf{H} \left(\sum_{l=1, l \neq k}^K \mathbf{X}^{(l)}\mathbf{U}^{(l)} \right) + \mathbf{Z}, \quad (2.2)$$

where $\mathbf{X}^{(l)}$ is the codeword matrix for the l -th user.

In (2.2), \mathbf{Z} is the complex i.i.d. Gaussian noise matrix with entries $\mathcal{CN}(0, N_0)$ and $\mathbf{H} \in \mathbb{C}^{n_R \times n_T}$ is the independent Rayleigh fading channel matrix with complex i.i.d. entries $\mathcal{CN}(0, 1)$, which is given by

$$\mathbf{H} = \begin{bmatrix} \mathbf{h}_1 \\ \mathbf{h}_2 \\ \vdots \\ \mathbf{h}_{n_R} \end{bmatrix} = \begin{bmatrix} h_{1,1} & h_{1,2} & \cdots & h_{1,n_T} \\ h_{2,1} & h_{2,2} & \cdots & h_{2,n_T} \\ \vdots & \vdots & \ddots & \vdots \\ h_{n_R,1} & h_{n_R,2} & \cdots & h_{n_R,n_T} \end{bmatrix}.$$

We assume that the channel matrix \mathbf{H} is constant during one STBC block and varies from one block to another independently.

2.3 STBCs for MIMO Multiuser systems

In this section, we first recall the rank and determinant criteria for STBC design. We show how to use TAST codes and perfect STBCs for the downlink of MIMO multiuser systems.

2.3.1 Rank and Determinant Criteria

For the k -th user, we assume that a codeword \mathbf{X} is transmitted. The maximum-likelihood receiver might decide erroneously in favor of another codeword $\hat{\mathbf{X}}$. Let r denote the rank of the codeword difference matrix $\mathbf{C} = \mathbf{X} - \hat{\mathbf{X}}$, and $\lambda_i, i = 1, \dots, r$, be the eigenvalues of the codeword distance matrix $\mathbf{A} = \mathbf{C}\mathbf{C}^\dagger$.

Then the pairwise error probability (PWE) is upper bounded by

$$P(\mathbf{X} \rightarrow \hat{\mathbf{X}}) \leq \left(\prod_{i=1}^r \lambda_i \right)^{-n_R} \left(\frac{E_s}{N_0} \right)^{-rn_R} \quad (2.3)$$

where E_s is the average energy of QAM information symbols and $\frac{E_s}{N_0}$ denotes the signal-to-noise ratio (SNR) per transmit antenna.

In (2.3), we call the minimum value of rn_R the diversity gain. We call the minimum value of $\left(\prod_{i=1}^r \lambda_i \right)^{1/r}$ the coding gain. In order to minimize the PWE, the rank and determinant criteria in [2] were proposed as follows:

- Rank Criterion: The minimum rank r of the codeword difference matrix should be maximized;
- Determinant Criterion: The minimum determinant $\prod_{i=1}^r \lambda_i$ should be maximized.

In our MIMO multiuser system, we consider the TAST and perfect STBCs that achieve full diversity $n_R n_T$ and full rate of n_T QAM symbols per channel use.

2.3.2 TAST Codes for the Downlink of Multiuser MIMO Systems

We recall TAST codes from [33]. The TAST codes are constructed by transmitting a scaled DAST code in each layer (or thread) l , where $l = 1, \dots, n_R$, i.e.

$$\mathbf{x}_l = \phi_l \mathbf{M} \mathbf{b}_l, \quad (2.4)$$

where \mathbf{x}_l are the encoded symbols, \mathbf{b}_l are the complex QAM symbol vectors defined in (2.1), and ϕ_l is chosen to ensure full diversity and maximize the coding gain of the component codes. In [33], ϕ_l is given by

$$\phi_l = \phi^{(l-1)/n_T}, \quad (2.5)$$

where $\phi = e^{i\lambda}$ and $\lambda \neq 0$ is either an algebraic number or transcendental number [33].

In (2.4), $\mathbf{M} \in \mathbb{C}^{n_T \times n_T}$ is a rotation matrix defining a DAST code. Let $\mathbf{s} = [s_1, \dots, s_{n_T}]^T = \mathbf{M} \mathbf{b}$ and $\hat{\mathbf{s}} = [\hat{s}_1, \dots, \hat{s}_{n_T}]^T = \mathbf{M} \hat{\mathbf{b}}$ be two different DAST codewords, where \mathbf{b} and $\hat{\mathbf{b}}$ are two different information symbol vectors. The rotation matrix \mathbf{M} is chosen to maximize the associated minimum product distance d_p , defined as [38],

$$d_p = \min_{\mathbf{s} \neq \hat{\mathbf{s}}} \prod_{i=1}^{n_T} |s_i - \hat{s}_i|. \quad (2.6)$$

Thus one can easily verify that DAST codes achieve full diversity, and their coding gains are proportional to the minimum product distance associated with the rotations used. The rotation matrix \mathbf{M} is constructed from an algebraic number field $\mathbb{Q}(\theta)$ of degree n_T [39, 33].

For L layers, where $L = n_R$ for the system in this paper, we can write the TAST codeword matrix as

$$\mathbf{X} = \sum_{l=1}^{n_R} (\phi_l \mathbf{e}^{l-1}) \text{diag}(\mathbf{M}\mathbf{b}_l), \quad (2.7)$$

where

$$\mathbf{e} = \begin{bmatrix} 0 & 1 & 0 & \cdots & 0 & 0 \\ \vdots & 0 & 1 & 0 & \cdots & 0 \\ \vdots & \vdots & \ddots & \ddots & \ddots & \vdots \\ 0 & 0 & 0 & 0 & 1 & 0 \\ 0 & 0 & 0 & 0 & \cdots & 1 \\ 1 & 0 & 0 & 0 & \cdots & 0 \end{bmatrix}. \quad (2.8)$$

2.3.3 Perfect STBCs for the Downlink of Multiuser MIMO Systems

For the special cases of $n_T = 3, 4, 6$, perfect STBCs was proposed in [36, 37]. The perfect STBCs are constructed based on cyclic division algebras, where the codeword is given by [36, 37],

$$\mathbf{X} = \sum_{l=1}^{n_T} \mathbf{e}^{l-1} \text{diag}(\mathbf{M}\mathbf{b}_l), \quad (2.9)$$

where

$$\mathbf{e} = \begin{bmatrix} 0 & 1 & 0 & \cdots & 0 \\ \vdots & 0 & 1 & 0 & \vdots \\ \vdots & & & \ddots & \vdots \\ 0 & 0 & 0 & 0 & 1 \\ \gamma & 0 & 0 & 0 & 0 \end{bmatrix}, \quad (2.10)$$

and γ is chosen from $\mathbb{Z}[j]$ in order to achieve the full diversity and non-vanishing determinant [36]. Comparing to TAST codes, we have a different \mathbf{e} matrix and $\phi = 1$.

In this case, we only consider subcodes of the perfect STBCs with a reduced number of layers n_R , i.e.,

$$\mathbf{X} = \sum_{l=1}^{n_R} \mathbf{e}^{l-1} \text{diag}(\mathbf{M}\mathbf{b}_l).$$

2.4 Lattice Decoder for the Downlink of MIMO Multiuser systems

The k -th user received signal matrix \mathbf{Y} in (2.2) is despread by multiplying \mathbf{U}^\dagger , which yields

$$\hat{\mathbf{Y}} = \mathbf{Y}\mathbf{U}^\dagger = \mathbf{H}\mathbf{X} + \hat{\mathbf{Z}}, \quad (2.11)$$

where

$$\hat{\mathbf{Y}} = \begin{bmatrix} \hat{y}_{1,1} & \hat{y}_{1,2} & \cdots & \hat{y}_{1,n_T} \\ \vdots & \vdots & \ddots & \vdots \\ \hat{y}_{n_R,1} & \hat{y}_{n_R,2} & \cdots & \hat{y}_{n_R,n_T} \end{bmatrix} \quad (2.12)$$

and

$$\hat{\mathbf{Z}} = \mathbf{Z}\mathbf{U}^\dagger = \begin{bmatrix} \hat{z}_{1,1} & \hat{z}_{1,2} & \cdots & \hat{z}_{1,n_T} \\ \vdots & \vdots & \ddots & \vdots \\ \hat{z}_{n_R,1} & \hat{z}_{n_R,2} & \cdots & \hat{z}_{n_R,n_T} \end{bmatrix}. \quad (2.13)$$

Let us define

$$\tilde{\mathbf{M}} = \mathbf{M} \otimes \mathbf{I}_{n_R} \quad \tilde{\mathbf{X}} = \tilde{\mathbf{M}} \times \text{vec}(\mathbf{B}), \quad (2.14)$$

where \otimes denotes matrix Kronecker product and

$$\text{vec}(\mathbf{B}) = \begin{bmatrix} \mathbf{b}_1 \\ \mathbf{b}_2 \\ \vdots \\ \mathbf{b}_{n_R} \end{bmatrix}. \quad (2.15)$$

Vectorizing (2.11) yields

$$\text{vec}(\hat{\mathbf{Y}}) = \text{vec}(\mathbf{H}\mathbf{X}) + \text{vec}(\hat{\mathbf{Z}}), \quad (2.16)$$

where

$$\text{vec}(\hat{\mathbf{Y}}) = [\hat{y}_{1,1}, \dots, \hat{y}_{1,n_T}, \dots, \hat{y}_{n_R,1}, \dots, \hat{y}_{n_R,n_T}]^T,$$

$$\text{vec}(\hat{\mathbf{Z}}) = [\hat{z}_{1,1}, \dots, \hat{z}_{1,n_T}, \dots, \hat{z}_{n_R,1}, \dots, \hat{z}_{n_R,n_T}]^T,$$

and $\text{vec}(\mathbf{H}\mathbf{X}) = \tilde{\mathbf{H}}\tilde{\mathbf{X}}$ is given in (2.17). For perfect STBC, \mathbf{e} is given in (2.10) and $\phi = 1$.

$$\text{vec}(\mathbf{H}\mathbf{X}) = \tilde{\mathbf{H}}\tilde{\mathbf{X}} = \begin{bmatrix} \text{diag}(\mathbf{h}_1) & (\text{diag}(\mathbf{h}_1)\phi\mathbf{e})^T & \cdots & (\text{diag}(\mathbf{h}_1)\phi^{n_R-1}\mathbf{e}^{n_R-1})^T \\ \vdots & \vdots & \ddots & \vdots \\ \text{diag}(\mathbf{h}_l) & (\text{diag}(\mathbf{h}_l)\phi\mathbf{e})^T & \cdots & (\text{diag}(\mathbf{h}_l)\phi^{n_R-1}\mathbf{e}^{n_R-1})^T \\ \vdots & \vdots & \ddots & \vdots \\ \text{diag}(\mathbf{h}_{n_R}) & (\text{diag}(\mathbf{h}_{n_R})\phi\mathbf{e})^T & \cdots & (\text{diag}(\mathbf{h}_{n_R})\phi^{n_R-1}\mathbf{e}^{n_R-1})^T \end{bmatrix} \begin{bmatrix} x_{1,1} \\ x_{1,2} \\ \vdots \\ x_{1,n_T} \\ \vdots \\ x_{l,1} \\ x_{l,2} \\ \vdots \\ x_{l,n_T} \\ \vdots \\ x_{n_R,1} \\ x_{n_R,2} \\ \vdots \\ x_{n_R,n_T} \end{bmatrix} \quad (2.17)$$

Substituting (2.14) and (2.17) into (2.16) yields

$$\text{vec}(\hat{\mathbf{Y}}) = \tilde{\mathbf{T}}\text{vec}(\mathbf{B}) + \text{vec}(\hat{\mathbf{Z}}), \quad (2.18)$$

where $\tilde{\mathbf{T}} = \tilde{\mathbf{H}}\tilde{\mathbf{M}}$.

Let us define

$$\mathcal{Y} = [\Re(\text{vec}(\hat{\mathbf{Y}})) \Im(\text{vec}(\hat{\mathbf{Y}}))]^T,$$

where $\Re(\cdot)$ and $\Im(\cdot)$ denote the real and imaginary part of the symbol vectors. Let us define

$$\mathcal{B} = [\Re(\text{vec}(\mathbf{B})) \Im(\text{vec}(\mathbf{B}))]^T$$

and

$$\mathcal{H} = \begin{bmatrix} \Re(\tilde{\mathbf{T}}) & -\Im(\tilde{\mathbf{T}}) \\ \Im(\tilde{\mathbf{T}}) & \Re(\tilde{\mathbf{T}}) \end{bmatrix}$$

Lattice decoding can be employed to decode the k -th user QAM symbols $\hat{\mathcal{B}}$, i.e.

$$\hat{\mathcal{B}} = \arg \min_{\mathbf{B} \in \mathcal{S}^n} \|\hat{\mathcal{Y}} - \mathcal{H}\hat{\mathcal{B}}\|^2, \quad (2.19)$$

where $n = 2 \times n_T \times n_R$.

Remark: The choice of the n_R layers within the codeword \mathbf{X} is irrelevant, since this corresponds to a permutation of the blocks in the matrix $\tilde{\mathbf{H}}$ which yields an equivalent code.

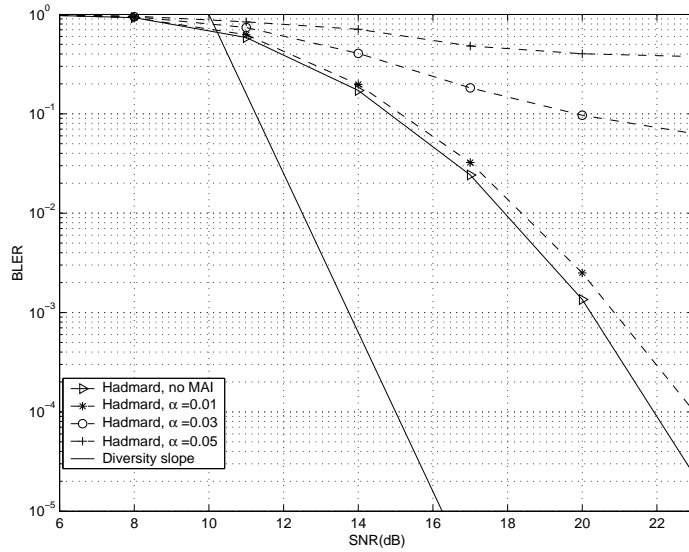


Figure 2.2: The Downlink of MIMO Multiuser System 1

2.5 Simulation Results

In the simulations, we show performance of the downlink MIMO system employing perfect STBCs. Performance is evaluated in terms of BLER by Monte Carlo simulation. The SNR per user is defined as $\text{SNR} = n_R E_s / N_0$. In the simulation, we consider two different systems as below.

System 1: We assume that the base station has four transmit antennas. There are two users, each of which has two receive antennas and 16-QAM symbols are used. We assume each STBC block consists of 8 symbols per user.

We choose 4×4 perfect STBC using two layers, where the rotation matrix \mathbf{M} is given in [36,37] and $\gamma^2 = -1$. This provides full diversity and highest possible rate of $n_R n_T = 8$ symbols per block per user. We choose Hadamard matrices as the spreading matrices.

Performance of System 1 is shown in Fig. 2 together with the diversity gain slope. Due to multipath propagation, different time delayed versions of the transmitted signal may result in MAI, which destroys the orthogonality of the spreading codes. In Fig. 2, we show the impact of MAI on the code performance. For User 1, after despreading, we have $\mathbf{U}^{(2)}\mathbf{U}^{(1)} = \alpha \mathbf{1}_{n_T}$, where the MAI interference coefficient is chosen to be $\alpha = 0.01, 0.03, 0.05$, respectively. We can see an error floor appears when $\alpha > 0$.

System 2: We assume that the base station has four transmit antennas. There are two users: User 1 has one receive antenna, User 2 has three receive antennas, and 16-QAM symbols are used.

The total transmission rate per block is 16 symbols. The transmitted codeword consists of one layer perfect STBC for User 1 (4 QAM symbols), and three layer perfect STBC for User 2 (12 QAM symbols). The performance of System 2 is shown in Fig. 3. We notice that User 2 achieves better performance at higher SNRs thanks to its receive

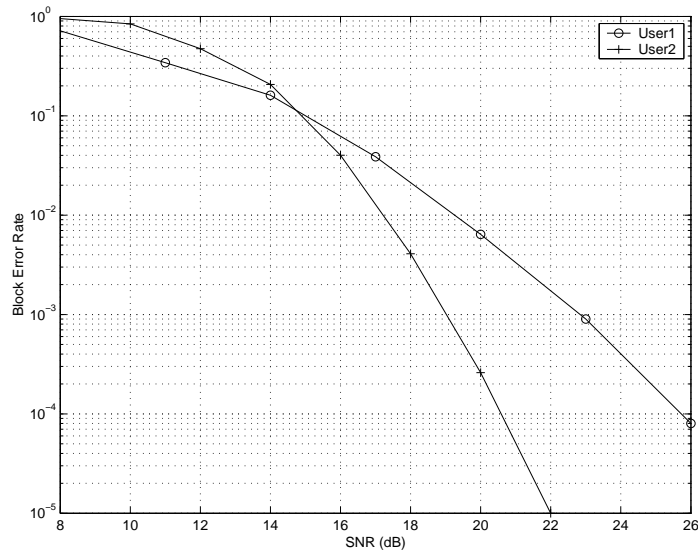


Figure 2.3: The Downlink of MIMO Multiuser System 2

antenna diversity, even if its rate is three times the rate of User 1.

Remarks: To the authors' knowledge, no comparable scheme was found in the literature for comparison. The proposed scheme offers great flexibility in the number of terminal receive antennas.

2.6 Conclusion

We consider space time block codes for the downlink of a multiuser MIMO system in this paper. We show how to use TAST block codes and perfect STBCs for such systems in order to achieve the highest possible transmission rate and full diversity gain. Orthogonal spreading matrices are used to separate the data streams of multiple users. At the receiver of each user, maximum likelihood decoding is obtained by using a lattice decoder. Performance of the space-time block coded system with different MAI is evaluated by simulations. It is shown that the system has good performance when the interference coefficient $\alpha = 0$, otherwise, an error floor appears. The proposed scheme is suitable to a network supporting different types of terminals due to its flexibility.

Chapter 3

Spatially Multiplexed LDPC Codes for Multi-User Detection

3.1 Introduction

Low-Density Parity-Check (LDPC) codes [44, 47] achieve rates close to channel capacity for a wide range of channels. The performance of these codes is optimized in function of the degree distributions of the bipartite graph associated with the LDPC code. This optimization can be performed exactly by using density evolution [49] (without assuming specific distributions for the messages) or approximately by using extrinsic information transfer (EXIT) charts [43] assuming that the messages have a Gaussian distribution.

If we aim to iterate over a multi-user detector and an error correcting code, we have to optimize the overall EXIT function of the code to match the EXIT function of the multi-user detector. The overall extrinsic information transfer function of a code optimized for the Gaussian memoryless channel is a step function [48]. This is consistent with the curve fitting approach of EXIT charts, since the extrinsic information transfer function of a memoryless Gaussian channel is constant and therefore, the best fit is achieved using a step function. On the other hand, for a multi-user detector, the EXIT function is not constant.

In Section 3.2 we introduce the system model and the multi-user detector. The EXIT functions of the multi-user detector are presented in Section 3.3 and the LDPC code design is described in Section 3.4. Finally, we present simulation results in Section 3.5.

3.2 System Description

We consider a receiver that performs iterative detection and decoding. The whole system can be represented by augmenting the factor graph [45] of the LDPC code with the elements of the multi-user detector as shown in Figure 3.1. The left part shows the LDPC decoder with check nodes of degree d_c and variable nodes of degree d_v . The right part corresponds to the multi-user detector, where every code symbol is repeated L times, which corresponds to the spreading length. Spreading is performed by multiplying a spreading sequence and the spreaded chips are interleaved over the complete block. This

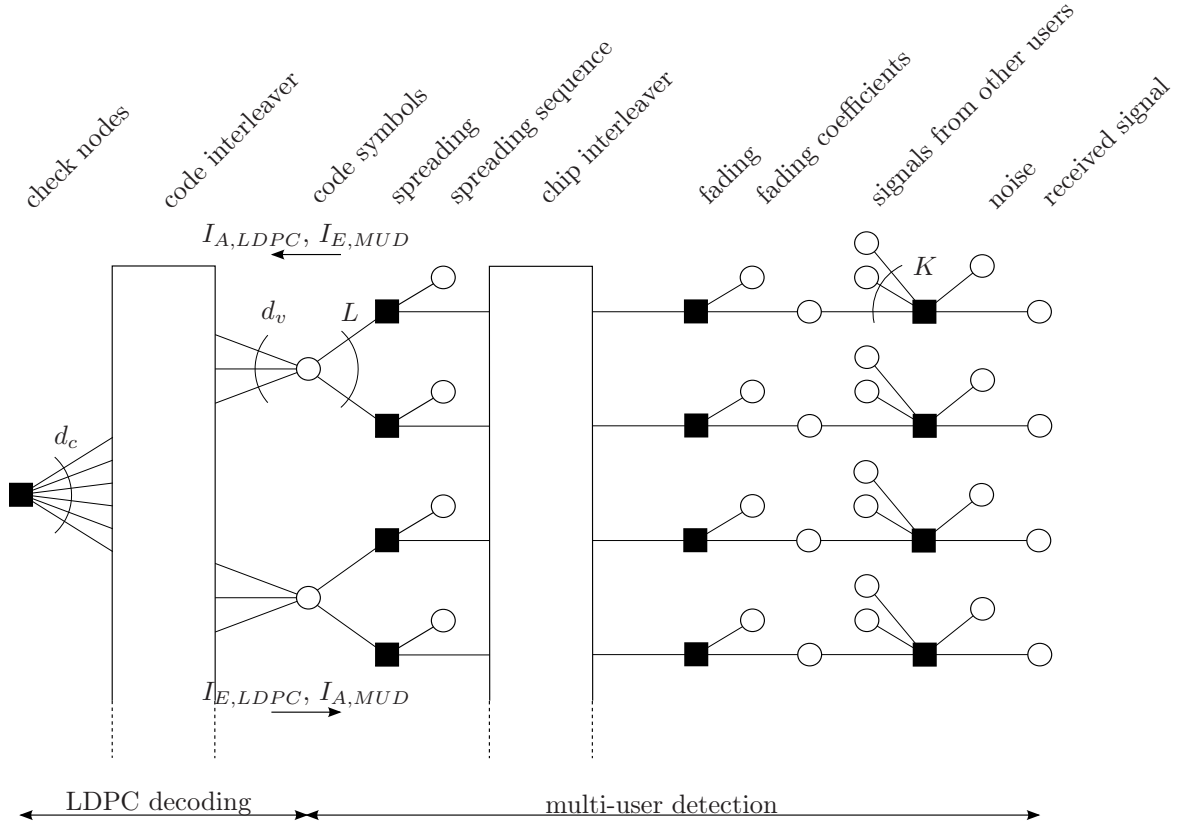


Figure 3.1: Factor graph for iterative multi-user detection and decoding.

has the advantage that chips corresponding to one code symbol are spread up in time which increases the diversity in the case of a slow fading channel. We will consider random spreading sequences which are not necessarily orthogonal but allow to operate the system overloaded. The chips are multiplied by the fading coefficients and the receiver observes the sum of the transmitted signals from K users plus white Gaussian noise.

3.2.1 Multi-User Detector

We focus on systems with low implementation complexity that are scalable in the number of users and in the spreading length. The optimal multi-user detector has a complexity that is exponential in the number of users. The multi-user detector presented in this section performs interference cancellation at chip level which can be implemented using a message passing algorithm avoiding the need of matrix multiplications and matrix inversions. Therefore, the system has a computational complexity which is linear in the number of users K as well as in the spreading length L .

Let \vec{c}_k denote the codeword of length N of user k with elements from $\{+1, -1\}$. The transmitter performs spreading followed by a chip-level interleaver. The whole process with spreading length L is described by a repeat code with encoder matrix \vec{G}_R of dimension $LN \times N$, the multiplication with a spreading sequence \vec{s}_k of length LN followed by a permutation that represents the chip-level interleaver as

$$\vec{x}_k = \vec{P}_k \cdot \text{diag}(\vec{s}_k) \cdot \vec{G}_R \cdot \vec{c}_k, \quad (3.1)$$

where \vec{x}_k denotes the signal transmitted by user k and \vec{P}_k is the permutation matrix of dimension $LN \times LN$.

The received signal \vec{y} is composed of the sum of all user signals and additive white Gaussian noise as

$$\vec{y} = \sum_{k=1}^K \left\{ \text{diag}(\vec{h}_k) \cdot \vec{x}_k \right\} + \vec{n}, \quad (3.2)$$

where \vec{h}_k contains the LN channel realizations of user k .

The multi-user detector performs interference cancellation on chip level for every user. The interference canceled vector \vec{z}_k is given by

$$\vec{z}_k = \vec{y} - \sum_{j=1; j \neq k}^K \left\{ \text{diag}(\vec{h}_j) \cdot \vec{P}_j \cdot \text{diag}(\vec{s}_j) \cdot \vec{G}_R \cdot \tanh \frac{\vec{L}_{a,j}}{2} \right\}, \quad (3.3)$$

where $\vec{L}_{a,j}$ denotes the a-priori log-likelihood ratios of the code symbols, that are provided by the LPDC decoder. The interference canceled vector \vec{z}_k is well approximated by a Gaussian distribution [51] with mean \vec{h}_k and variance

$$\vec{\sigma}_{z,k}^2 = \sigma_n^2 + \sum_{j=1; j \neq k}^K \left(1 - \left(\tanh \frac{\vec{L}_{a,j}}{2} \right)^2 \right). \quad (3.4)$$

This allows us to express the log-likelihood ratios \vec{L}_k as

$$\vec{L}_k = 2 \cdot \vec{z}_k \text{diag}(\vec{h}_k) \cdot \text{diag}(\vec{\sigma}_{z,k}^2)^{-1}. \quad (3.5)$$

Finally, decoding of the repeat code \vec{G}_R is performed by summing up the corresponding log-likelihood ratios after despreading and deinterleaving

$$\vec{L}_{e,k} = \vec{G}_R^T \cdot \text{diag}(\vec{s}_k) \cdot \vec{P}_k^T \cdot \vec{L}_k, \quad (3.6)$$

resulting in a vector $\vec{L}_{e,k}$ that is passed to the LDPC decoder to complete the iterative detection and decoding process. In addition to performing only one iteration at the multi-user detector, the system can be modified by allowing the multi-user detector to perform more than one iteration between the code symbols and the received signal.

In the rest of this paper, we will assume a flat fading channel where the fading coefficients are constant during one symbol, i.e. during L chips, and are independently taken from a Rayleigh distribution. Furthermore, we assume that the receiver has perfect knowledge of the channel realizations.

3.3 EXIT Functions

We use extrinsic information transfer (EXIT) [43] functions to analyze the behavior of the multi-user detector and design an LDPC code for the system. For this purpose, we

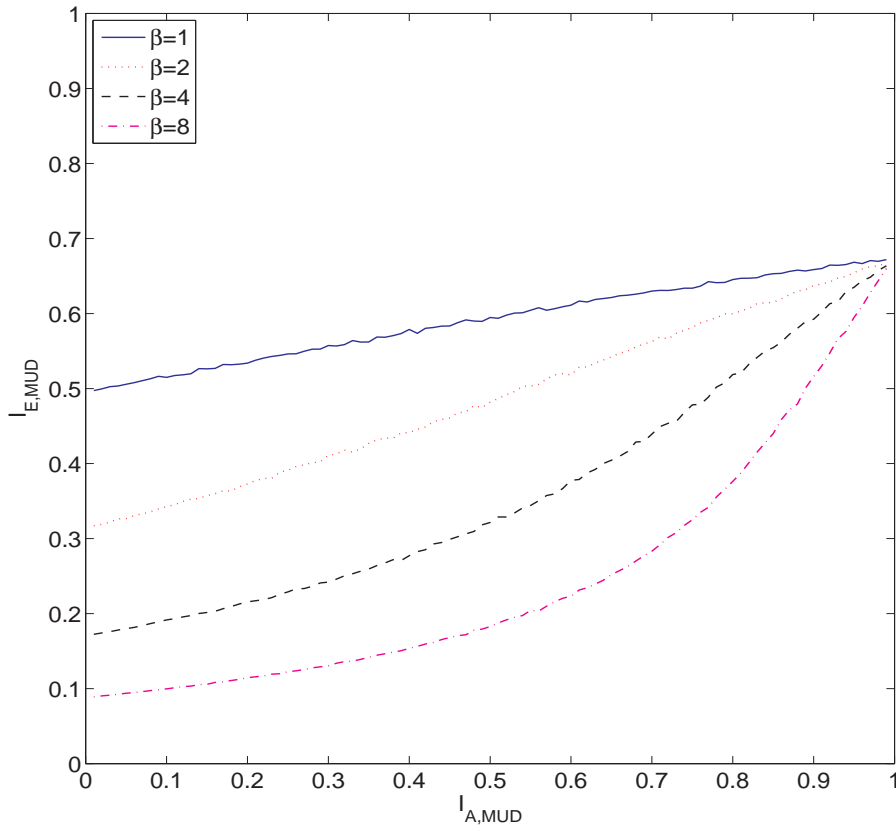


Figure 3.2: EXIT functions of multi-user detector as a parameter of the system load for $L = 4$ and $E_s/N_0 = 0.0\text{dB}$.

investigate how the EXIT function of the multi-user detector depends on the parameters of the system.

In Figure 3.2 we show the dependency of the EXIT function on the system load $\beta = K/L$ which were obtained using Monte Carlo simulations. The functions are plotted for the system loads of 1, 2, 4 and 8 at a signal to noise ratio $E_s/N_0 = 0.0\text{dB}$, where E_s denotes the energy per transmitted code symbol, i.e. the energy per L chips. The spreading length was $L = 4$ and the multi-user detector was allowed to perform five iterations. It can be observed that for small values of $I_{A,MUD}$ the EXIT curve is dominated by the multi-user interference. In contrast, for $I_{A,MUD}$ approaching 1.0, the EXIT curve becomes independent of the system load since the other users are perfectly known and can be canceled.

To analyze the dependency on the signal to noise ratio, we fixed the system load at $\beta = 4$ and simulated the EXIT function of the multi-user detector for increasing signal to noise ratio shown in Figure 3.3. For small values of $I_{A,MUD}$ the influence of the signal to noise ratio is quite small, whereas for large values of $I_{A,MUD}$, the EXIT curve is only a function of the signal to noise ratio.

For low signal to noise ratio and/or low system load, the EXIT function of the multi-user detector approaches a horizontal line, i.e. it becomes independent of the a-priori

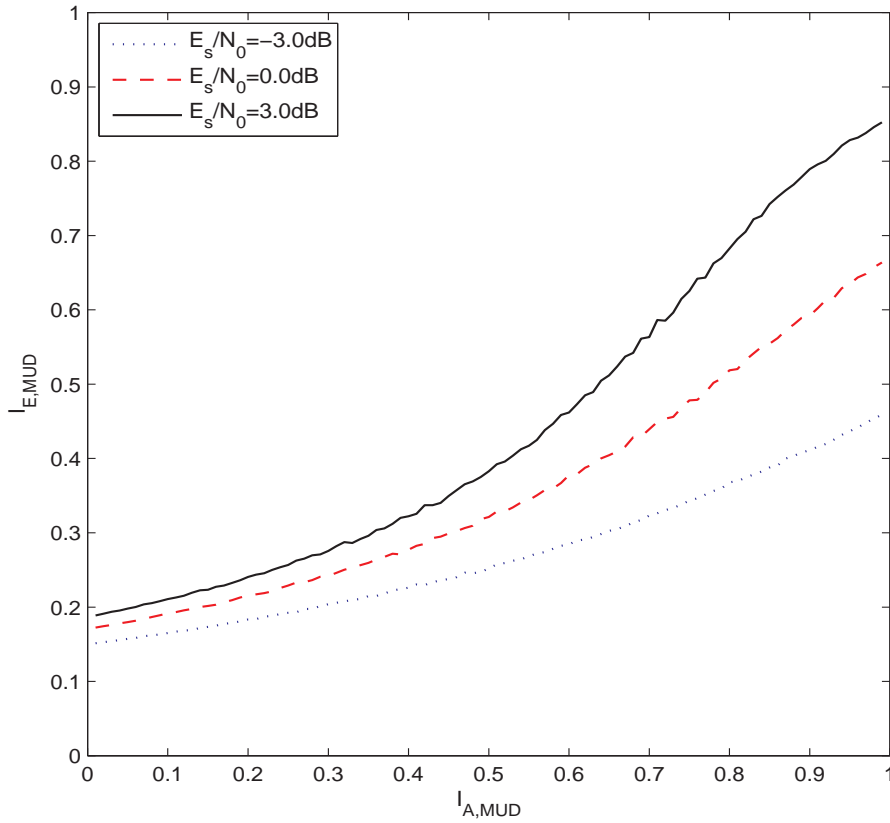


Figure 3.3: EXIT functions of multi-user detector as a parameter of the signal to noise ratio for $L = 4$ and $\beta = 4$.

information provided by the LDPC decoder. In this scenario, the multi-user channel can be treated as a single user Gaussian channel (i.e. the noise interference is much stronger than the interference of the other users) and error correcting codes optimized for Gaussian channels can be used. In all other cases, codes have to be designed for a specific system load and signal to noise ratio in order to approach the capacity of the multi-user channel.

3.3.1 Coding versus Spreading

To compare systems with different parameters we compute the spectral efficiency [50]

$$C = \frac{K}{L}R = \beta R, \quad (3.7)$$

where R denotes the rate of the error correcting code. The maximum spectral efficiency for a given load is achieved when the rate of the error correcting code is equal to the capacity C_u for every user. The overall redundancy in the system is split up into spreading (i.e. a repeat code of length L) and into the redundancy added by the LDPC code. To answer the question, how this redundancy should be divided into coding and spreading, we evaluate the spectral efficiency of the system parametrized by the system load. For this purpose

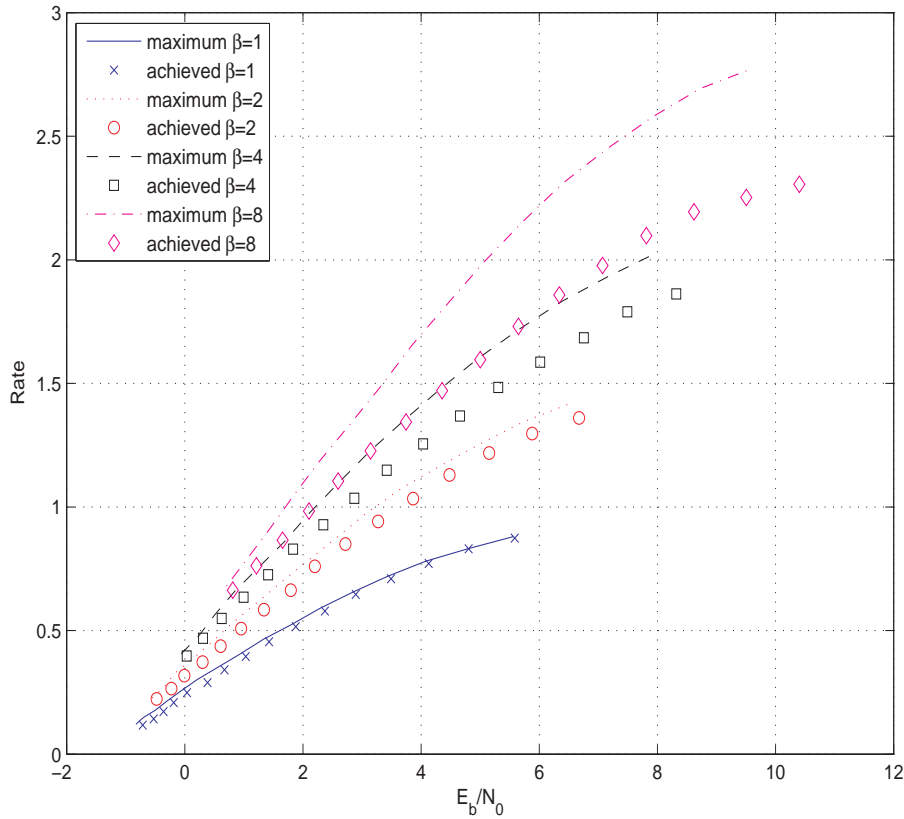


Figure 3.4: Spectral efficiency and results of code optimization.

we use the area property of EXIT functions [43], which states that the area below the EXIT function is equivalent to the capacity if the a-priori information is modeled as being transmitted over a binary erasure channel. This area corresponds to the capacity C_u for every user.

The maximum achievable spectral efficiency is shown in Figure 3.4 for system loads of 1, 2, 4 and 8 as a function of E_b/N_0 . It can be observed, that the spectral efficiency increases with increasing system load. Therefore, from a theoretical point of view, all the redundancy should be spent for coding and no spreading should be performed.

However, not using spreading results in a EXIT function of the multi-user detector that depends heavily on the number of users in the system which is equivalent to the system load in the case of no spreading. From a practical point of view, spreading can be used to keep the system load approximately constant and design an LDPC code for this load.

3.3.2 Multiple Transmit Antennas

The performance of a multi-user system can be improved by allowing the users to transmit using more than one antenna. The system described in Section 3.2, is then modified so that the interleaved chips are partitioned onto the individual transmit antennas. From

the point of view of the multi-user detector, this increases the load since it treats every single antenna as a separate user. Besides the effect of increased diversity, this is beneficial for the performance of the system since higher system loads can achieve a higher spectral efficiency as shown in the previous section.

3.4 LDPC Code Design

To optimize the code (i.e. maximizing the code rate for a given signal to noise ratio), we use the methods presented in [46]. In order to get codes with practical parameters, we restricted the variable node degree distribution to three non-zero parameters (2, 3 and 10) and set the maximum check node degree to 30. The optimization of the variable node degree distribution was performed by an exhaustive search while for every distribution, the check node degree distribution was optimized using linear programming [46]. The resulting achieved spectral efficiency of the designed systems is shown in Figure 3.4. Systems with higher load always outperform those with smaller load. For small loads the achieved spectral efficiency of the designed systems is close to the maximum achievable spectral efficiency. For increasing load and increasing signal to noise ratio, the gap increases. The reason for that is, that the shape of the EXIT function of the multi-user detector can not be matched by the LDPC code with the given parameters (see for example, the EXIT function at $E_s/N_0 = 3.0\text{dB}$ in Figure 3.3).

3.5 Simulation Results

To verify our derivations, we designed a system for a load of $\beta = 4$ and a spectral efficiency of 1.0, leading to a code rate $R = 0.25$. The EXIT functions of the multi-user detector and the optimized LDPC code for this system are shown in Figure 3.5. From the EXIT chart analysis, the threshold of this system is at $E_b/N_0 = 2.75\text{dB}$. We constructed a random LDPC code with the given degree distributions and a block length of $N = 10^4$. The bit error rate simulation shown in Figure 3.6 shows that the simulation agrees with the EXIT chart prediction. In Figure 3.5 we also plotted the EXIT function of an LDPC code that was optimized for an AWGN channel [42]. This system can not converge for the given load since the EXIT functions always intersect (even for the case of very large signal to noise ratio).

3.6 Conclusion

We showed how the EXIT function of a multi-user detector depends on the load and the signal to noise ratio. By using the area property of EXIT charts, we compared the achievable spectral efficiency of systems of different loads. For the case where the multi-user interference is stronger than the interference caused by Gaussian noise, an LDPC code optimized for this scenario can significantly outperform a standard LDPC code that is optimized for an AWGN channel.

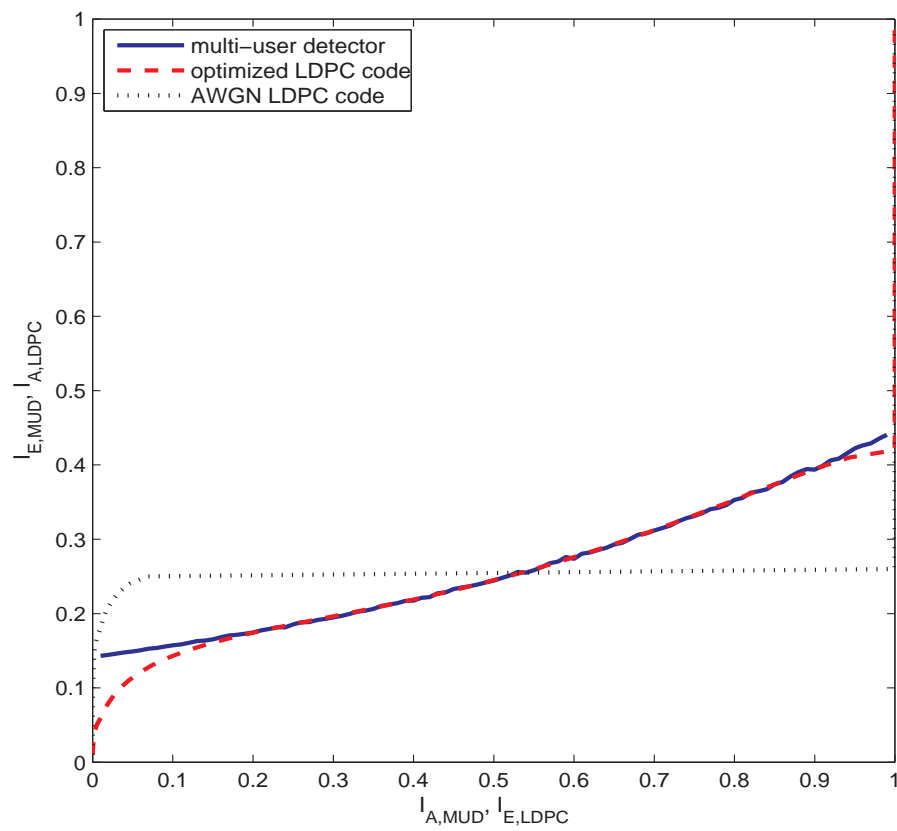


Figure 3.5: EXIT function of multi-user detector and LDPC decoder for $\beta = 4$ and $E_b/N_0 = 2.75\text{dB}$.

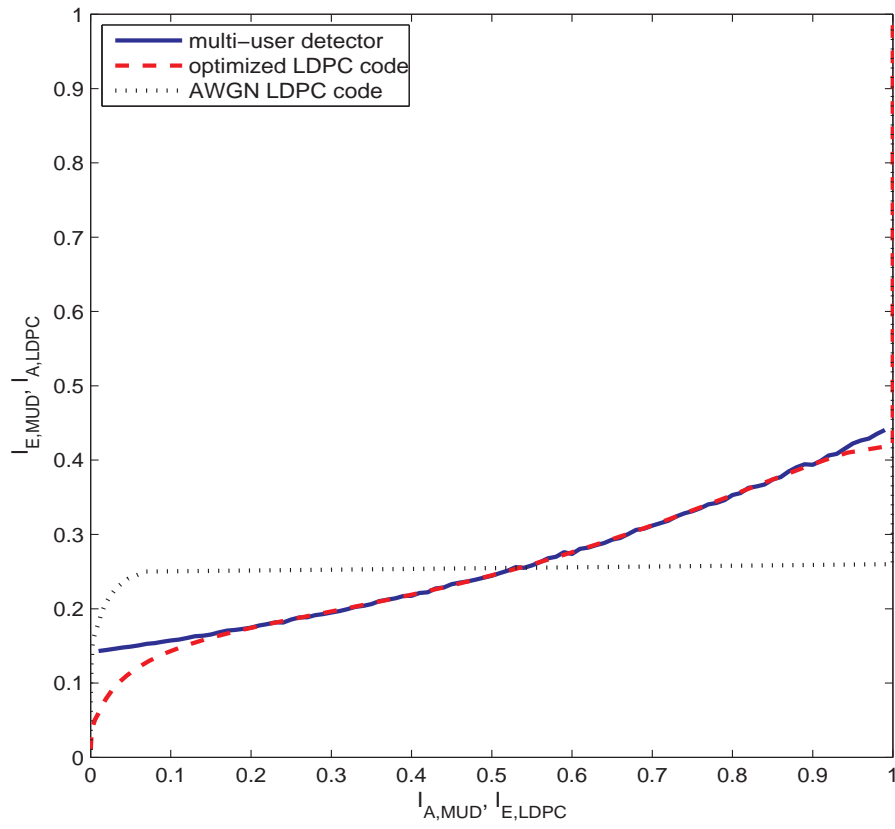


Figure 3.6: Bit error rate simulation for design example.

Chapter 4

MU-MIMO Uplink Using IDMA and Low-Complexity Iterative Receivers

4.1 Introduction

In multiuser communications, CDMA is widely used for multiple access because of its attractive properties. With CDMA, user separation is obtained through signature (spreading) sequences, and fading effects are combated by an interleaver placed between the forward error correction (FEC) coding and the spreading. The performance of CDMA systems is limited by multiple-access interference (MAI) and intersymbol interference (ISI) [52]. Because of the high complexity of optimal joint detection and decoding, sub-optimal receiver techniques are commonly used. A turbo-type receiver where the multiuser detector and the channel decoders exchange extrinsic information [53] has been presented in [?]. This receiver uses soft interference cancellation by means of an MMSE filter.

In [54], *interleave-division multiple access* (IDMA) has been proposed and demonstrated to outperform coded CDMA when iterative receivers are used. IDMA employs user-specific interleavers combined with low-rate channel coding for user separation. It is a wideband scheme that allows the use of multiuser detectors with significantly lower complexity compared to the CDMA case. IDMA shares with CDMA several desirable features, especially diversity against fading and mitigation of user interference from other cells [54].

In this paper, we generalize IDMA to multiple-antenna (MIMO) multiuser systems in which the users employ spatial multiplexing [10] to achieve high data rates. The resulting *MIMO-IDMA* scheme extends all advantages of IDMA to the MIMO case. Furthermore, generalizing the receiver proposed in [54], we develop an iterative receiver for MIMO-IDMA that employs an efficient soft multiuser detector whose complexity is linear in the number of users. Both flat-fading and frequency-selective MIMO channels are considered.

The paper is organized as follows. In Section 4.2, we describe the structure of the new MIMO-IDMA system, including the iterative receiver. The MIMO-IDMA soft multiuser detector is developed on Section 4.3. Finally, simulation results demonstrating the performance of MIMO-IDMA are presented in Section 4.4.

4.2 The Proposed MIMO-IDMA System

4.2.1 Basic System Model

We consider an uplink multiple-access scenario where each user (transmitter) has M_T antennas and employs spatial multiplexing [10], and the base station (receiver) has M_R antennas. The MIMO channel is allowed to be time-varying and frequency-selective. At a given time instant n , the received vector $\mathbf{r}[n] = (r_1[n] \cdots r_{M_R}[n])^T$ can thus be expressed as

$$\mathbf{r}[n] = \sum_{m=1}^M \sum_{l=0}^{L-1} \mathbf{H}^{(m)}[n, l] \mathbf{x}^{(m)}[n-l] + \mathbf{w}[n], \quad (4.1)$$

where $\mathbf{x}^{(m)}[n] = (x_1^{(m)}[n] \cdots x_{M_T}^{(m)}[n])^T$ is the data vector transmitted by the m th user, $\mathbf{H}^{(m)}[n, l]$ is the $M_R \times M_T$ MIMO channel matrix from the m th user to the base station (l denotes the discrete delay), $\mathbf{w}[n] = (w_1[n] \cdots w_{M_R}[n])^T$ is a noise vector, L is the channel length, and M is the number of users. We assume that the data symbols $x_k^{(m)}[n]$ are drawn from a BPSK alphabet $\mathcal{A} = \{-1, 1\}$ and the elements of the noise vector $\mathbf{w}[n]$ are i.i.d. Gaussian with variance σ^2 .

4.2.2 MIMO-IDMA Transmitter

The proposed MIMO-IDMA transmitter extends the IDMA transmitter of [54] to the multiuser MIMO spatial multiplexing case. As shown in Fig. 4.1(a), the data bit sequence of the m th user, $\mathbf{b}^{(m)} = (b^{(m)}[1] \cdots b^{(m)}[K])^T$, is encoded into a code bit sequence $\mathbf{c}^{(m)} = (c^{(m)}[1] \cdots c^{(m)}[N])^T$. Here, $N = K/R$ where R is the code rate. The code is a serial concatenation of a terminated convolutional code for FEC and a low-rate repetition code.

Next, the code bit sequence $\mathbf{c}^{(m)}$ is interleaved by a user-specific interleaver $\pi^{(m)}(\cdot)$, resulting in the sequence $\mathbf{d}^{(m)}$ with $d^{(m)}[n] = c^{(m)}[\pi^{(m)}(n)]$. The M interleavers are assumed to be randomly generated. The repeat code together with the user-specific interleaver performs a kind of spreading, somewhat similar to the spreading in a CDMA system. Finally, the interleaved bit sequence is BPSK-modulated using the mapping $0 \rightarrow -1, 1 \rightarrow 1$ and split into blocks of length M_T to yield the symbol vector $\mathbf{x}^{(m)}[n]$ transmitted by the M_T transmit antennas. The combined action of the BPSK mapping and serial-to-parallel conversion is expressed by

$$\mathbf{x}^{(m)}[n] = \begin{pmatrix} 2d^{(m)}[nM_T + 1] - 1 \\ 2d^{(m)}[nM_T + 2] - 1 \\ \vdots \\ 2d^{(m)}[(n+1)M_T] - 1 \end{pmatrix}, \quad n = 0, \dots, \frac{N}{M_T} - 1. \quad (4.2)$$

4.2.3 Iterative MIMO-IDMA Receiver

The structure of the iterative (turbo-type [53, ?, 54]) MIMO-IDMA receiver is shown in Fig. 4.1(b). The receiver consists of two stages: a low-complexity soft MIMO multiuser

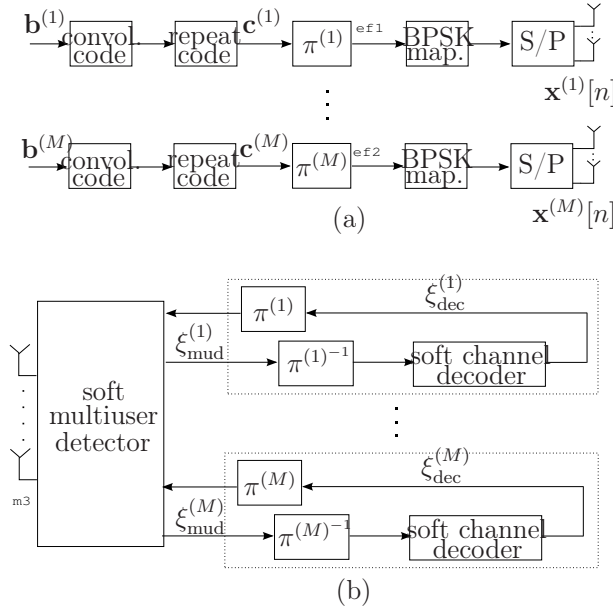


Figure 4.1: *The proposed MIMO-IDMA system: (a) Transmitter, (b) receiver.*

detector—to be developed in the next section—is followed by M parallel single-user soft-in/soft-out channel decoders (one corresponding to each user). These two stages are connected via deinterleavers and interleavers and exchange soft-information, as described in the following.

Soft MIMO Multiuser Detection. Assuming independent interleaved symbols $d^{(m)}[n]$ (i.e., ignoring the code dependencies), a symbolwise operation of the multiuser detector is optimum. At a given iteration, the detector then estimates the *a posteriori* log-likelihood ratio (LLR) of the code bits $c^{(m)}[n]$,

$$\ell_{\text{mud}}(c^{(m)}[n]) \triangleq \log \frac{P(c^{(m)}[n] = 1 | \tilde{\mathbf{r}})}{P(c^{(m)}[n] = 0 | \tilde{\mathbf{r}})}, \quad (4.3)$$

for $n = 1, \dots, N$ and $m = 1, \dots, M$. Here, $\tilde{\mathbf{r}}$ denotes the sequence of all received vectors $\mathbf{r}[n]$. In what follows, we will often suppress the dependence on n for simplicity of notation, e.g., we will write $c^{(m)}$ instead of $c^{(m)}[n]$. With Bayes' rule, (4.3) can be rewritten as

$$\ell_{\text{mud}}(c^{(m)}) = \log \frac{P(\tilde{\mathbf{r}} | c^{(m)} = 1)}{P(\tilde{\mathbf{r}} | c^{(m)} = 0)} + \log \frac{P(c^{(m)} = 1)}{P(c^{(m)} = 0)}. \quad (4.4)$$

The first term is the *extrinsic information* delivered by the MIMO multiuser detector and will be denoted as $\xi_{\text{mud}}(c^{(m)})$:

$$\xi_{\text{mud}}(c^{(m)}) \triangleq \log \frac{P(\tilde{\mathbf{r}} | c^{(m)} = 1)}{P(\tilde{\mathbf{r}} | c^{(m)} = 0)}. \quad (4.5)$$

Since according to (4.2) $x_k^{(m)}[n]$ corresponds to $d^{(m)}[nM_T + k] = c^{(m)}[\pi^{(m)}(nM_T + k)] =: c_{\pi,k}^{(m)}[n]$ via the BPSK mapping, the extrinsic information for $x_k^{(m)}[n]$ equals that for $c_{\pi,k}^{(m)}[n]$, i.e., $\xi_{\text{mud}}(x_k^{(m)}) = \xi_{\text{mud}}(c_{\pi,k}^{(m)})$. The second term in (4.4) is the *a priori* LLR of $c^{(m)}$. An estimate of this term is provided by the channel decoder of the m th user at the previous iteration. For the first iteration, equally likely bits are assumed, i.e., the *a priori* LLR values are set to zero. Finally, the sequence of extrinsic informations $\xi_{\text{mud}}(c^{(m)}[n])$ is deinterleaved by the deinterleaver of the m th user and fed into the corresponding soft channel decoder as *a priori* information for the next iteration. The detailed operation of the soft MIMO multiuser detector will be described in the Section 4.3.

Soft Channel Decoding. The channel decoder for the m th user estimates the *a posteriori* LLR of the code bits

$$\ell_{\text{dec}}(c^{(m)}) = \log \frac{P(c^{(m)} = 1 | \tilde{\mathbf{r}})}{P(c^{(m)} = 0 | \tilde{\mathbf{r}})},$$

based on the extrinsic information from the multiuser detector, $\xi_{\text{mud}}(c^{(m)})$, and the code structure. To estimate $\ell_{\text{dec}}(c^{(m)})$, the repeat code is soft-decoded by summing the *a priori* LLR values of the appropriate symbols (this presupposes that the corresponding received symbols are independent due to the combined action of the interleaver and the noisy fading channel), while the convolutional code is soft-decoded by the BCJR algorithm [55]. As in (4.4), $\ell_{\text{dec}}(c^{(m)})$ can be expressed as the sum of an extrinsic information $\xi_{\text{dec}}(c^{(m)})$ and an *a priori* LLR [?]. The sequence of extrinsic informations $\xi_{\text{dec}}(c^{(m)}[n])$ is interleaved and fed back to the multiuser detector as *a priori* information for the next iteration. Additionally, the channel decoder estimates the *a posteriori* LLRs of the information bits; at the final iteration, it performs a decision on the information bits by applying the sign function.

4.3 A Low-Complexity Soft Multiuser Detector for MIMO-IDMA

We will now develop a low-complexity soft multiuser detector for MIMO-IDMA. As discussed above, the purpose of the soft multiuser detector is to calculate the extrinsic informations $\xi_{\text{mud}}(c_{\pi,k}^{(m)})$ based on the current received vector \mathbf{r} and the extrinsic informations $\xi_{\text{dec}}(x_k^{(\nu)})$, $\nu = 1, \dots, M$ produced by the channel decoders at the previous iteration. Our development extends the IDMA soft multiuser detector of [54] to the MIMO spatial-multiplexing case.

4.3.1 Flat-Fading Channel

For simplicity, we first consider a flat-fading channel; the frequency-selective case will be considered in the next subsection. In the flat-fading case, (4.1) simplifies to

$$\mathbf{r}[n] = \sum_{m=1}^M \mathbf{H}^{(m)}[n] \mathbf{x}^{(m)}[n] + \mathbf{w}[n]. \quad (4.6)$$

This can be formulated as (again, we omit the time instant n)

$$\mathbf{r} = \mathbf{h}_k^{(m)} x_k^{(m)} + \boldsymbol{\eta}_k^{(m)}. \quad (4.7)$$

Here, $\mathbf{h}_k^{(m)}$ is the k th column of $\mathbf{H}^{(m)}$ and $\boldsymbol{\eta}_k^{(m)}$ consists of the interference from the symbols transmitted from all other antennas of the same user, the interference from all other users, and the noise, i.e.,

$$\boldsymbol{\eta}_k^{(m)} = \sum_{\substack{j=1 \\ j \neq k}}^{M_T} \mathbf{h}_j^{(m)} x_j^{(m)} + \sum_{\substack{\nu=1 \\ \nu \neq m}}^M \mathbf{H}^{(\nu)} \mathbf{x}^{(\nu)} + \mathbf{w}.$$

Development of the Multiuser Detector. The proposed MIMO-IDMA multiuser detector is based on the assumption that $\boldsymbol{\eta}_k^{(m)}$ has a Gaussian distribution; this will be approximately true for a large number of users. For given user channels $\mathbf{H}^{(m)}$, the conditional probability density function of \mathbf{r} given $x_k^{(m)}$ then is

$$p(\mathbf{r}|x_k^{(m)}) \sim \mathcal{N}\left(\mathbf{h}_k^{(m)} x_k^{(m)} + \mathbb{E}(\boldsymbol{\eta}_k^{(m)}), \mathbf{C}_{\boldsymbol{\eta}_k^{(m)}}\right),$$

where $\mathbb{E}(\boldsymbol{\eta}_k^{(m)})$ and $\mathbf{C}_{\boldsymbol{\eta}_k^{(m)}}$ denote, respectively, the mean and covariance matrix of $\boldsymbol{\eta}_k^{(m)}$ for given user channels $\mathbf{H}^{(m)}$. Using the Gaussian assumption, the extrinsic information in (4.5) becomes

$$\xi_{\text{mud}}(c_{\pi,k}^{(m)}) = \xi_{\text{mud}}(x_k^{(m)}) = 2\mathbf{h}_k^{(m)H} \mathbf{C}_{\boldsymbol{\eta}_k^{(m)}}^{-1} [\mathbf{r} - \mathbb{E}(\boldsymbol{\eta}_k^{(m)})], \quad (4.8)$$

which is recognized as the MMSE estimate of $x_k^{(m)}$ from \mathbf{r} using the linear model (4.7).

It remains to calculate $\mathbb{E}(\boldsymbol{\eta}_k^{(m)})$ and $\mathbf{C}_{\boldsymbol{\eta}_k^{(m)}}$. Inserting (4.6) into (4.7) yields $\boldsymbol{\eta}_k^{(m)} = \sum_{\nu=1}^M \mathbf{H}^{(\nu)} \mathbf{x}^{(\nu)} - \mathbf{h}_k^{(m)} x_k^{(m)} + \mathbf{w}$ and, thus,

$$\mathbb{E}(\boldsymbol{\eta}_k^{(m)}) = \sum_{\nu=1}^M \mathbf{H}^{(\nu)} \mathbb{E}(\mathbf{x}^{(\nu)}) - \mathbf{h}_k^{(m)} \mathbb{E}(x_k^{(m)}). \quad (4.9)$$

Furthermore, from (4.7) we obtain

$$\mathbf{C}_{\boldsymbol{\eta}_k^{(m)}} = \mathbf{C}_r - \mathbf{h}_k^{(m)} \text{var}(x_k^{(m)}) \mathbf{h}_k^{(m)H}. \quad (4.10)$$

Here, \mathbf{C}_r is the covariance matrix of the received vector \mathbf{r} , given by

$$\mathbf{C}_r = \sum_{m=1}^M \mathbf{H}^{(m)} \mathbf{C}_{x^{(m)}} \mathbf{H}^{(m)H} + \sigma^2 \mathbf{I}, \quad (4.11)$$

with $\mathbf{C}_{x^{(m)}} = \text{diag}\{\text{var}(x_k^{(m)})\}_{k=1, \dots, M_T}$ (this expression is

based on the assumption that, due to the interleaver, the symbols $x_k^{(m)}[n]$ are independent). Woodbury's identity [56] gives the following expression of $\mathbf{C}_{\eta_k^{(m)}}^{-1}$:

$$\mathbf{C}_{\eta_k^{(m)}}^{-1} = \mathbf{C}_r^{-1} - \mathbf{C}_r^{-1} \mathbf{h}_k^{(m)} \left[\mathbf{h}_k^{(m)H} \mathbf{C}_r^{-1} - \frac{1}{[\text{var}(x_k^{(m)})]^2} \right] \mathbf{h}_k^{(m)H} \mathbf{C}_r^{-1}. \quad (4.12)$$

Thus, computation of (4.8) only requires a single matrix inversion.

Finally, we express $\mathbb{E}(x_k^{(m)})$ and $\text{var}(x_k^{(m)})$ in terms of $\xi_{\text{dec}}(x_k^{(m)})$. In the iterative receiver scheme, the extrinsic information $\xi_{\text{dec}}(x_k^{(m)})$ produced by the channel decoders at the previous iteration is substituted for the *a priori* LLR of $c_{\pi,k}^{(m)}$ (recall that $x_k^{(m)}$ corresponds to $c_{\pi,k}^{(m)}$ via the BPSK mapping), i.e.,

$$\log \frac{P(c_{\pi,k}^{(m)}=1)}{P(c_{\pi,k}^{(m)}=0)} \stackrel{!}{=} \xi_{\text{dec}}(x_k^{(m)}).$$

This is easily seen to imply the expressions

$$\mathbb{E}(x_k^{(m)}) = \tanh \frac{\xi_{\text{dec}}(x_k^{(m)})}{2}, \quad \text{var}(x_k^{(m)}) = 1 - [\mathbb{E}(x_k^{(m)})]^2.$$

Complexity. The complexity of the proposed multiuser detector (using (4.12)) is linear in the number of users M . It is furthermore cubic in the number of receive antennas M_R because (4.12) requires inversion of the $M_R \times M_R$ matrix \mathbf{C}_r .

Scheduling Strategies. The updating of the *a priori* information at the input of the multiuser detector can be done in two different ways [57]. With *parallel scheduling*, the *a priori* information of all users at the input of the multiuser detector is updated by the channel decoders and used to calculate the extrinsic information of all users at the output of the multiuser detector concurrently. With *serial scheduling*, only the *a priori* information of one user is updated at a time and used to calculate the extrinsic information of all users at the output of the multiuser detector. In the next time step, the *a priori* information of another user is updated, and so forth.

4.3.2 Frequency-Selective Channel

Again generalizing [54], we now extend the MIMO-IDMA multiuser detector developed above to frequency-selective channels, i.e., channels introducing ISI. According to (4.1),

the channel of the m th user is characterized by $\mathbf{H}^{(m)}[n, l]$, where $l \in \{0, \dots, L-1\}$. To take ISI into account, we combine L successive received vectors into the super-vector $\bar{\mathbf{r}}[n] \triangleq (\mathbf{r}[n] \ \mathbf{r}[n+1] \ \dots \ \mathbf{r}[n+L-1])^T$ of length $M_R L$. Using (4.1), we can formulate $\bar{\mathbf{r}}[n]$ as

$$\bar{\mathbf{r}}[n] = \bar{\mathbf{h}}_k^{(m)}[n] x_k^{(m)}[n] + \bar{\boldsymbol{\eta}}_k^{(m)}[n]. \quad (4.13)$$

Here, $\bar{\mathbf{h}}_k^{(m)}[n] \triangleq (\mathbf{h}_k^{(m)}[n, 0] \ \mathbf{h}_k^{(m)}[n+1, 1] \ \dots \ \mathbf{h}_k^{(m)}[n+L-1, L-1])^T$, where $\mathbf{h}_k^{(m)}[n, l]$ is the k th column of $\mathbf{H}^{(m)}[n, l]$, and $\bar{\boldsymbol{\eta}}_k^{(m)}[n] \triangleq (\boldsymbol{\eta}_k^{(m)}[n] \ \boldsymbol{\eta}_k^{(m)}[n+1] \ \dots \ \boldsymbol{\eta}_k^{(m)}[n+L-1])^T$. Because (4.13) has the form of the linear model (4.7), the extrinsic information $\xi_{\text{mud}}(c_{\pi,k}^{(m)})$ can be calculated as in (4.8) with obvious modifications:

$$\xi_{\text{mud}}(c_{\pi,k}^{(m)}) = \xi_{\text{mud}}(x_k^{(m)}) = 2\bar{\mathbf{h}}_k^{(m)H} \mathbf{C}_{\bar{\boldsymbol{\eta}}_k^{(m)}}^{-1} [\bar{\mathbf{r}} - \mathbf{E}(\bar{\boldsymbol{\eta}}_k^{(m)})],$$

with $\mathbf{E}(\bar{\boldsymbol{\eta}}_k^{(m)})$ and $\mathbf{C}_{\bar{\boldsymbol{\eta}}_k^{(m)}}$ given by equations (4.9)–(4.12) suitably modified. The complexity still is linear in M and cubic in M_R ; it is furthermore cubic in the channel's impulse response length L .

4.4 Simulation results

We next present simulation results demonstrating the performance of the proposed MIMO-IDMA system.

Flat-fading channel. We first consider the case of a fast time-varying flat-fading channel. We simulated a MIMO-IDMA system with $M = 16$ users, $M_T = 4$ antennas per user, $M_R = 4$ base station antennas, and a terminated rate- $\frac{1}{2}$ convolutional code (code polynomial $[23 \ 35]_8$) serially concatenated with a rate- $\frac{1}{16}$ repetition code (thus, the overall code rate was $R = \frac{1}{32}$). The number of information bits per block was $K = 128$; this implies a total number of $K/(RM_T) = 1024$ transmit vectors per user. The channel matrices $\mathbf{H}^{(m)}[n]$ of size 4×4 were generated independently for each n , with elements that were i.i.d. Gaussian with zero mean and unit variance. The multiuser detector used parallel scheduling.

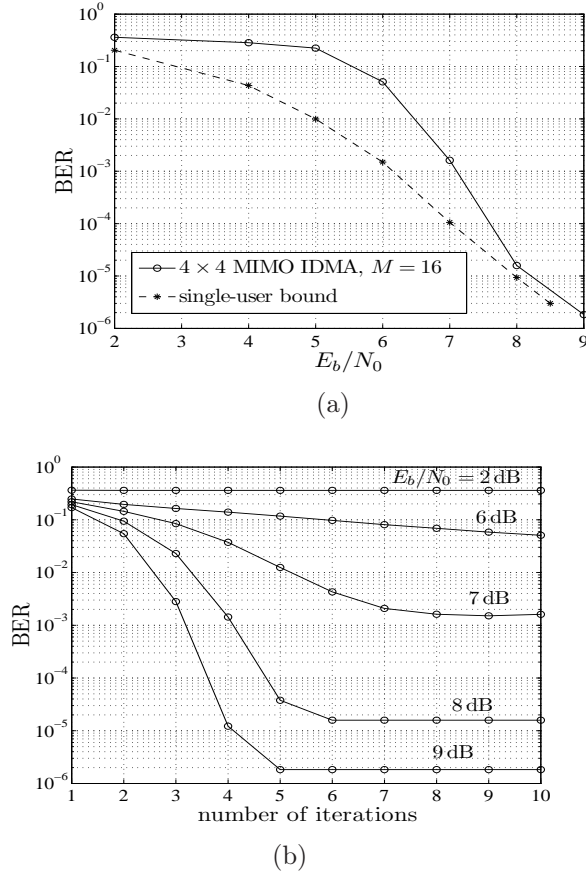


Figure 4.2: Performance of a 4×4 MIMO-IDMA system with 16 users for a fast time-varying flat-fading channel. (a) Averaged BER versus E_b/N_0 and single-user bound after 10 iterations. (b) Averaged BER versus the number of iterations, parametrized by E_b/N_0 .

In Fig. 4.2(a), the BER averaged over all users after 10 iterations is shown versus the SNR E_b/N_0 (we note that $E_b/N_0 = M_T/(R\sigma^2)$). The single-user bound (BER for one user, i.e., $M = 1$) is shown as a performance reference. It is seen that the BER of the multiuser system approaches the single-user bound for high SNR. In Fig. 4.2(b), the convergence of the iterative receiver, i.e., BER as a function of the number of iterations, is depicted for various values of E_b/N_0 . It is seen that the system converges for E_b/N_0 larger than about 7 dB. For higher E_b/N_0 , the convergence is faster and the BER after convergence is lower. For high E_b/N_0 (about 9 dB), the receiver converges after about 5 iterations.

Frequency-selective channel. Next, we consider a time-varying frequency-selective channel with $L = 3$ taps. The channel was generated such that it stays constant for 50 transmit vectors and then a new realization is drawn independently. Because the matrices now have threefold size, a smaller system with MIMO dimension 2×2 and $M = 8$ users was implemented to reduce simulation times. All other system parameters were as before. Fig. 4.3 shows the BER as a function of E_b/N_0 after 20 iterations. The gap to the single-user bound is smaller compared to the flat-fading case because of the smaller number of users and the delay diversity offered by the frequency-selective channel.

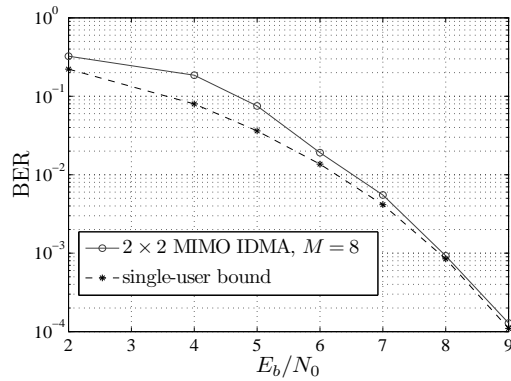


Figure 4.3: BER of a 2×2 MIMO-IDMA system with 8 users versus E_b/N_0 for a time-varying frequency-selective channel.

4.5 Conclusions

We proposed a MIMO-IDMA system for uplink multiuser communications over frequency-selective channels. This system generalizes the IDMA system described in [54] to the MIMO spatial multiplexing case. It uses a turbo-type iterative MIMO-IDMA receiver incorporating an efficient soft MIMO multiuser detector whose complexity is linear in the number of antennas.

MIMO-IDMA is attractive due to its good performance and low complexity. The basic MIMO-IDMA system considered here can be extended in various ways. The simple convolutional code can be replaced by more sophisticated codes such as LDPC codes [49]. Various strategies for selecting the order of the users in the serial scheduling scheme described in Subsection 4.3.1 can be used. A detailed assessment of the performance and complexity of these and other variants of MIMO-IDMA in comparison to a CDMA-based multiuser MIMO system will be pursued in the course of our future research.

Chapter 5

Conclusions and Recommendation

This deliverable provides the detailed technical contributions with specific targetting at various coding schemes for multiuser MIMO systems, multiuser data transmissison, multiuser detection and decoding.

Chapter 1 provides the general space-time/frequency code design criteria for fading multiantenna MACs with perfect channel state information at the receiver. The essence of our design criteria is to recognize that, depending on the transmission rate tuple, joint code designs may or may not be necessary. It was shown that joint designs essentially require applying the classical design criteria [2, 3, 4] to a sum of codeword difference matrices, with the specific sum depending on the subset of users leading to the dominant error event for the given transmission rate tuple. Systematic joint code designs constitute an interesting area of future research. Chapter 1 also investigates the outage probability and the diversity-multiplexing tradeoff for the case of general Ricean fading MIMO channels. This is potentially useful for many real-world wireless scenarios.

Chapter 2 successfully explored a space-time block coded transmission scheme for multiuser MIMO downlinks. This scheme has the advantage of supporting the highest possible users and full diversity of the multiuser MIMO systems, yet with low encoding and decoding complexity.

Chapters 3 considers the practical issues of the multi-user detection for synchronous CDMA with various system loads and SNRs. The evaluation tool is based on Extrinsic information transfer function (EXIT) charts. Also, good low-density parity-check codes are designed for the CDMA system.

Chapter 4 extends the IDMA system to MIMO cases which can successfully exploit the spatial multiplexing gains. A detailed assessment of the performance and complexity of MIMO-IDMA in comparison to a CDMA-based multiuser MIMO system will be pursued in the future research.

Bibliography

- [1] D. S. Baum, D. A. Gore, R. U. Nabar, S. Panchanathan, K. V. S. Hari, V. Erceg, and A. J. Paulraj, "Measurement and characterization of broadband MIMO fixed wireless channels at 2.5 GHz," in *Proc. IEEE Int. Conf. Personal Wireless Communications (ICPWC)*, Hyderabad, India, Dec. 2000, pp. 203–206.
- [2] V. Tarokh, N. Seshadri, and A. R. Calderbank, "Space-time codes for high data rate wireless communication: Performance criterion and code construction," *IEEE Trans. Inform. Theory*, vol. 44, no. 2, pp. 744–765, Mar. 1998.
- [3] H. Bölcskei and A. J. Paulraj, "Space-frequency coded broadband OFDM systems," in *Proc. IEEE Wireless Commun. Netw. Conf. (WCNC)*, vol. 1, Chicago, IL, Sept. 2000, pp. 1–6.
- [4] B. Lu and X. Wang, "Space-time code design in OFDM systems," in *Proc. IEEE Global Telecommun. Conf. (GLOBECOM)*, vol. 2, San Francisco, CA, Nov. 2000, pp. 1000–1004.
- [5] A. Paulraj, R. Nabar, and D. A. Gore, *Introduction to Space-Time Wireless Communications*. Cambridge, UK: Cambridge Press, 2003.
- [6] B. K. Ng and E. S. Sousa, "On bandwidth-efficient multiuser-space-time signal design and detection," *IEEE J. Select. Areas Commun.*, vol. 20, no. 2, pp. 320–329, Feb. 2002.
- [7] A. F. Naguib, N. Seshadri, and A. R. Calderbank, "Applications of space-time block codes and interference suppression for high capacity and high data rate wireless systems," in *Proc. Asilomar Conf. Signals, Syst., Comput.*, vol. 2, Pacific Grove, CA, Nov. 1998, pp. 1803–1810.
- [8] R. G. Gallager, "A perspective on multiaccess channels," *IEEE Trans. Inform. Theory*, vol. 31, no. 2, pp. 124–142, Mar. 1985.
- [9] A. Peled and A. Ruiz, "Frequency domain data transmission using reduced computational complexity algorithms," in *Proc. IEEE Int. Conf. Acoust., Speech, Signal Process. (ICASSP)*, vol. 5, Denver, CO, 1980, pp. 964–967.
- [10] D. N. C. Tse and P. Viswanath, *Fundamentals of Wireless Communication*. Cambridge, UK: Cambridge Press, 2005.
- [11] S. Visuri and H. Bölcskei, "Multiple-access strategies for frequency-selective MIMO channels," *IEEE Trans. Inform. Theory*, vol. 52, no. 9, pp. 3980–3993, Sept. 2006.
- [12] R. G. Gallager, *Information Theory and Reliable Communication*. New York: Wiley & Sons, 1968.
- [13] H. Boche and E. A. Jorswieck, "Outage probability of multiple antenna systems: Optimal transmission and impact of correlation," in *Proc. Int. Zurich Seminar Commun.*, Zürich, Switzerland, Feb. 2004, pp. 116–119.
- [14] A. W. Marshall and I. Olkin, *Inequalities: Theory of Majorization and Its Applications*. New York: Academic Press, 1979.

- [15] S. M. Alamouti, "A simple transmitter diversity scheme for wireless communications," in *IEEE J. Select. Areas Commun.*, vol. 16, no. 8, Oct. 1998, pp. 1451–1458.
- [16] I. E. Telatar, "Capacity of multi-antenna Gaussian channels," *Eur. Trans. Telecommun.*, vol. 10, no. 6, pp. 585–595, Nov. 1995.
- [17] G. J. Foschini and M. J. Gans, "On limits of wireless communications in a fading environment when using multiple antennas," *Wireless Personal Commun.*, vol. 6, no. 3, pp. 311–335, Mar. 1998.
- [18] E. A. Jorswieck and H. Boche, "Outage probability in multiple antenna systems," *Eur. Trans. Telecommun.*, vol. 18, no. 3, pp. 217–233, Apr. 2007.
- [19] M. R. McKay and I. B. Collings, "General capacity bounds for spatially correlated Rician MIMO channels," *IEEE Trans. Inform. Theory*, vol. 51, no. 9, pp. 3121–3145, Sept. 2005.
- [20] D. Höslı and A. Lapidoth, "How good is an isotropic Gaussian input on a MIMO Rician channel?" in *Proc. IEEE Int. Symp. Inform. Theory (ISIT)*, Chicago, IL, June 2004, p. 288.
- [21] D. Höslı, Y.-H. Kim, and A. Lapidoth, "Monotonicity results for coherent MIMO Rician channels," *IEEE Trans. Inform. Theory*, vol. 51, no. 12, pp. 4334–4339, Dec. 2005.
- [22] G. Alfano, A. Lozano, A. M. Tulino, and S. Verdú, "Mutual information and eigenvalue distribution of MIMO Ricean channels," in *Proc. Int. Symp. Inform. Theory and Appl. (ISITA)*, Parma, Italy, Oct. 2004, pp. 1040–1045.
- [23] G. Lebrun, M. Faulkner, M. Shafi, and P. J. Smith, "MIMO Ricean channel capacity: An asymptotic analysis," *IEEE Trans. Wireless Commun.*, vol. 5, no. 6, pp. 1343–1350, June 2006.
- [24] R. U. Nabar, H. Bölcskei, and A. J. Paulraj, "Diversity and outage performance in space-time block coded Ricean MIMO channels," *IEEE Trans. Wireless Comm.*, vol. 4, no. 5, pp. 2519–2532, Sept. 2005.
- [25] R. A. Horn and C. R. Johnson, *Matrix Analysis*, 1st ed. Cambridge, UK: Cambridge Press, 1985.
- [26] K. Scharnhorst, "Angles in complex vector spaces," *Acta Appl. Math.*, vol. 69, no. 1, pp. 95–103, Oct. 2001.
- [27] L. Zheng and D. N. C. Tse, "Diversity and multiplexing: A fundamental tradeoff in multiple-antenna channels," *IEEE Trans. Inform. Theory*, vol. 49, no. 5, pp. 1073–1096, May 2003.
- [28] A. M. Mathai and S. B. Provost, *Quadratic Forms in Random Variables: Theory and Applications*. New York: Marcel Dekker, 1992.
- [29] T. W. Anderson, *An Introduction to Multivariate Statistical Analysis*, 2nd ed. New York, NY: Wiley & Sons, 1984.
- [30] V. Tarokh, H. Jafarkhani and A. R. Calderbank, "Space-time block codes from orthogonal designs," *IEEE Transactions on Information Theory*, vol. 45, no. 5, pp. 1456–1467, July 1999.
- [31] M. O. Damen, K. Abed-Meraim, and J.-C. Belfiore, "Diagonal algebraic space-time block codes," *IEEE Transactions on Information Theory*, vol. 48, pp. 628–636, Mar. 2002.
- [32] M. O. Damen, K. Abed-Meraim, and J.-C. Belfiore, "Transmit diversity using rotated constellations with Hadamard transform," *IEEE Proc. 2000 Symp. Adaptive Systems for Signal Processing, Communications, and Control*, AB, Canada, pp. 396–401, Oct. 2000.
- [33] H. El Gamal and M. O. Damen, "Universal space-time codes," *IEEE Transactions on*

Information Theory, vol. 49, no. 5, pp. 1097-1119, May 2003.

- [34] B. A. Sethuraman, B. S. Rajan, and V. Shashidhar, "Full-diversity, high-rate space-time block codes from division algebras," *IEEE Transactions on Information Theory*, vol. 49, pp. 2596-2616, Oct. 2003.
- [35] J.-C. Belfiore, G. Rekaya, and E. Viterbo, "The Golden Code: A 2×2 full-rate space-time code with non-vanishing determinants," *IEEE Transactions on Information Theory*, vol. 51, no. 4, pp. 1432-1436, Apr. 2005.
- [36] G. Rekaya, J.-C. Belfiore, and E. Viterbo, "Algebraic 3×3 , 4×4 and 6×6 space-time codes with non-vanishing determinants," *IEEE proceedings of International Symposium on Information Theory and its applications*, Parma, Italy, pp. 325-329, Oct. 2004.
- [37] F. Oggier, G. Rekaya, J.-C. Belfiore, and E. Viterbo, "Perfect space time block codes," to appear in *IEEE Transactions on Information Theory*, April. 2006.
- [38] X. Girand, E. Boutillon, and J.-C. Belfiore, "Algebraic tools to build modulation schemes for fading channels," *IEEE Transactions on Information Theory*, vol. 43, pp. 938-952, May 1997.
- [39] J. Boutros and E. Viterbo, "Signal space diversity: a power and bandwidth efficient diversity technique for the Rayleigh fading channel," *IEEE Transactions on Information Theory*, vol. 44, pp. 1453-1467, July 1998.
- [40] F. Oggier and E. Viterbo, "Algebraic number theory and code design for Rayleigh fading channels," *Foundations and Trends in Communications and Information Theory*, vol. 1, pp. 333-415, 2004.
- [41] L. T. Berger and L. Schumacher, "Modified space-time transmission in DS-CDMA down-link facilitating MISO channel equalization," *IEEE 56th Vehicular Technology Conference*, Vancouver, BC, Canada, vol. 2, pp. 941-945, Sept. 2002.
- [42] "LDPC - a fast and accurate degree distribution optimizer for LDPC code ensembles," <http://lthcwwww.epfl.ch/research/ldpcopt/>.
- [43] A. Ashikhmin and G. Kramer and S. ten Brink, "Extrinsic information transfer functions: model and erasure channel properties," *Information Theory, IEEE Transactions on*, vol. 50, no. 11, Nov. 2004, pp. 2657 - 2673.
- [44] R. G. Gallager, "Low Density Parity Check Codes," MIT Press, 1963.
- [45] F. R. Kschischang and B. J. Frey, and H.-A. Loeliger, "Factor graphs and the sum-product algorithm," *Information Theory, IEEE Transactions on*, vol. 47, no. 2, Feb. 2001, pp. 498-519.
- [46] G. Lechner and J. Sayir, and I. Land, "Optimization of LDPC Codes for Receiver Frontends," *Proc. ISIT 2006, International Symposium on Information Theory, Seattle, USA*, June-July, 2006.
- [47] D.J.C. Mackay, "Good error-correcting codes based on very sparse matrices", *IEEE Transactions on Information Theory*, vol. 45, no. 2, Mar. 1999, pp. 399-431.
- [48] M. Peleg, and A. Sanderovich, and S. Shamai "On Extrinsic Information of Good Codes Operating Over Discrete Memoryless Channels," to appear in *European Transactions on Telecommunications (ETT)*, 2007.
- [49] T. Richardson and A. Shokrollahi and R. Urbanke, "Design of capacity-approaching irregular low-density parity-check codes," *IEEE Transactions on Information Theory*, vol. 47, Feb. 2001, pp. 619-637.

- [50] S. Verdú and S. Shamai, “Spectral efficiency of CDMA with random spreading”, *IEEE Transactions on Information Theory*, vol. 45, no. 2, pp. 622–640, March 1999.
- [51] Xiaodong Wang and H.V. Poor, “Iterative (turbo) soft interference cancellation and decoding for coded CDMA”, *IEEE Transactions on Communications*, vol. 47, no. 7, July 1999, pp. 1046–1061.
- [52] S. Verdú, “Multiuser Detection”, *Cambridge (UK)*, 1998.
- [53] P. H. Siegel and D. Divsalar and E. Eleftheriou and J. Hagenauer and D. Rowitch and W. H. Tranter, Eds., “The turbo principle: from theory to practice”, in *IEEE J. Sel. Areas Comm. Special Issue*, vol. 19, May 2001.
- [54] Li Ping and Lihai Liu and Keying Wu W.K. Leung, “Interleave-Division Multiple-Access”, in *IEEE Trans. on Wireless Commun.*, vol. 5, no. 4, pp. 938–947, April 2006.
- [55] L. R. Bahl and J. Cocke and F. Jelinek and J. Raviv, “Optimal decoding of linear codes for minimizing symbol error rate”, in *IEEE Trans. on Information Theory*, vol. 20, March 1974.
- [56] L. L. Scharf, “Statistical Signal Processing”, in *Addison Wesley*, Reading (MA), 1991.
- [57] J. Boutros and G. Caire, “Iterative multiuser joint decoding: Unified framework and asymptotic analysis”, *IEEE Transactions on Information Theory*, vol. 48, pp. 1772–1793, July 2002.